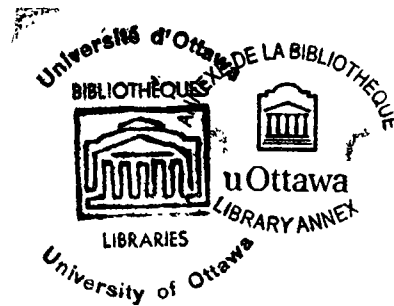


UNIVERSITY OF OTTAWA

SOME OBSERVATIONS ON BEACH SEDIMENT MOVEMENT
UNDER ICE AND OPEN WATER CONDITIONS AT THE
SOUTHERN END OF KLUANE LAKE, YUKON TERRITORY

ANDREW L. SILVER

Thesis submitted to the School of Graduate Studies
of the University of Ottawa in partial fulfillment
of the requirements for the degree of Master of
Arts in Geography and Regional Planning.



1976

UMI Number: EC55557

INFORMATION TO USERS

The quality of this reproduction is dependent upon the quality of the copy submitted. Broken or indistinct print, colored or poor quality illustrations and photographs, print bleed-through, substandard margins, and improper alignment can adversely affect reproduction.

In the unlikely event that the author did not send a complete manuscript and there are missing pages, these will be noted. Also, if unauthorized copyright material had to be removed, a note will indicate the deletion.

UMI[®]

UMI Microform EC55557
Copyright 2011 by ProQuest LLC
All rights reserved. This microform edition is protected against
unauthorized copying under Title 17, United States Code.

ProQuest LLC
789 East Eisenhower Parkway
P.O. Box 1346
Ann Arbor, MI 48106-1346

ABSTRACT

Field observations and data collection of sediment movement by ice and wave energy conditions were carried out at two sites on Kluane Lake. A program of observation and descriptive measurement was established during the 1975 ice breakup season on the lake, and its results were compared with documented features of other environments. It was found that although there is no permanent alteration of the beach form through ice action, many micro-relief features did develop during this period.

Measurements of wave characteristics, longshore velocity, and longshore sediment transport rate were taken during the remainder of the 1975 field season. Data on wave characteristics of height, period, and angle of approach were compiled by methods similar to the Littoral Environment Observation program developed by the Coastal Engineering Research Center, and longshore current velocity was determined by timing the rate of measurement alongshore of an identifiable object through a measured distance. These data were tested by comparing predicted and observed longshore current velocities. The predicted velocity was calculated from an equation developed with data from marine environments by Longuet-Higgins (1970) which was based upon the radiation stress theory previously developed by Longuet-Higgins and Stewart (1964). It was found at Kluane Lake that with a fixed value for the coefficient of friction, the correlation of predicted and observed longshore current velocities was between 0.5 to 0.6 whereas with a variable coefficient of friction there was near perfect correlation. Therefore, friction may play a more important role in

determining longshore current velocity in lower energy environments.

Longshore sediment transport velocities were gauged by placing marked sediment grains at one end of a known distance and timing their rate of movement. This velocity was converted into an immersed weight transport rate per unit length and compared with the longshore component of energy flux of the incoming waves. It was found that the wave energy at Kluane Lake ranged from threshold sediment movement to steady state, and the relationship between immersed weight transport rate to energy within these bounds tended to be curvilinear.

RESUME

Des travaux de terrain et des mesures du mouvement des sédiments par la glace et les vagues ont été faits à deux endroits le long du Lac Kluane.

Un programme d'observation et de mesures a été mis en place pendant la fonte des glaces en 1975 et les données obtenues ont été comparées à des résultats existants pour d'autres environnements. Il ne semble pas y avoir de formes permanentes créées par l'action des vagues mais, cependant, **beaucoup de micro-formes se développent pendant la fonte des glaces.**

Le reste de la saison de terrain 1975 a été consacré à des mesures de caractéristiques de vagues, de la vitesse de la dérive littorale et du taux de transport de sédiments le long du rivage. Les mesures de caractéristiques des vagues: hauteur, période, angle d'incidence ont été recueillies avec des méthodes similaires à celles utilisées par le programme de "littoral environmental observation" mis au point par le "Coastal Engineering Research Center". Les vitesses du courant de dérive littorale **ont été mesurées en chronométrant** le temps de déplacement d'un objet sur une distance connue. Ces données ont été testées par comparaison avec des valeurs calculées et observées. Les valeurs calculées ont été générées au moyen d'une équation empirique mise au point par Longuet-Higgins (1970) avec des données de milieux marins. Au Lac Kluane, avec une valeur fixe de coefficient de friction, la corrélation entre les valeurs calculées et les valeurs observées varie de 0.5 à 0.6, alors qu'avec le coefficient de friction variable, la corrélation est presque parfaite. La friction jouerait donc un rôle beaucoup plus important sur la

vitesse du courant de dérive littorale dans un milieu à plus basse énergie.

Les vitesses de déplacement de sédiments ont été évaluées en plaçant des sédiments marqués et en mesurant leur temps de déplacement sur une distance connue. Cette vitesse a été transformée en taux de transport d'un poids sous eau par unité de longueur et comparée avec la composante littorale de flux énergétique des vagues. Cette énergie des vagues au Lac Kluane varie entre le seuil de transport des sédiments et l'état d'équilibre. La relation entre le taux de transport d'un poids sous eau et l'énergie, entre ces deux limites, tend vers une courbe.

ACKNOWLEDGEMENTS

I wish to express my appreciation to Dr. P.G. Johnson for his supervision and helpful guidance through my tenure at the University of Ottawa, and to Professor D.A. St. Onge of the Department of Geography and Regional Planning and Professor R.G. Warnock of the Department of Civil Engineering, both of the University of Ottawa, and Mr. D. Willis of the Hydraulics Research Branch of the National Research Council for their suggestions and advice through the analysis and writing of this thesis. I would also like to express personal gratitude to my family for their words of encouragement through the entire project.

Also, a note of thanks is given to Nicole Racine for the splendid job of typing and to Carol Ullman for her help with the diagrams and figures.

Finally, I would like to thank the Northern Research Group of the University of Ottawa and the Arctic Institute of North America for their financial support enabling the research to be carried out for two field seasons in the Yukon, and special thanks to Andy Williams, Phil Upton, and the many other friends at the AINA base camp who gave invaluable help in the field data collection.

TABLE OF CONTENTS

ABSTRACT.	ii
RESUME.	iv
ACKNOWLEDGEMENTS.	vi
TABLE OF CONTENTS	vii
LIST OF FIGURES	viii
LIST OF TABLES.	ix
LIST OF PLATES.	x
LIST OF SYMBOLS	xi

CHAPTERS

1	INTRODUCTION.	1
2	SEDIMENT DISTURBANCE BY LAKE ICE.	17
3	NEARSHORE WATER DYNAMICS.	45
4	LONGSHORE SEDIMENT TRANSPORT BY WAVE ACTION	67
5	CONCLUSIONS	86
	REFERENCES	89

LIST OF FIGURES

1	Kluane Lake, Yukon Territory	3
2	AINA Beach Profile	12
3	Silver City Beach Profile.	13
4	Classification and description of ice-cover in formation .	19
5	Classification and description of ice-cover during breakup and melt at Kluane Lake.	23
6	Definition of terms.	46
7	Water particle displacements from mean position for shallow- water and deep water waves	48
8	The change of wave length and wave height in relation to the ratio of depth to wave length.	50
9	Wave refraction patterns	51
10	Schematic diagram of rip currents.	54
11	Definition of variables of a breaking wave	56
12	Relationship between observed and computed longshore current velocities	66
13	Terminology of nearshore current systems	68
14	Schematic diagram of longshore sediment movement	68
15	Relationship between immersed weight transport rate and longshore energy flux -- 9 mm sediment size.	83
16	Relationship between immersed weight transport rate and longshore energy flux -- 4 mm sediment size.	84
17	Relationship between immersed weight transport rate and longshore energy flux -- 2 mm sediment size.	85

LIST OF TABLES

1	AINA beach sediment sorting characteristics	14
2	Silver City beach sediment sorting characteristics.	15
3	Dimensions of ice floes and corresponding ice-push ridges . . .	41
4	Sediment sorting characteristics of ice push ridges I and II. .	42
5	Wave observations data, AINA beach site	63
6	Summary of data for calculation of predicted longshore current velocities AINA beach site.	65
7	Tracer grain velocities and rate of movement of a volume of sediment over a unit length	80
8	Coefficient of proportionality between immersed weight transport rate to longshore energy flux	81

LIST OF PLATES

1	AINA beach site	9
2	Silver City beach site.	10
3	Silver City beach sediment.	10
4	Sheet ice Floes	20
5	Sheet ice crystals.	20
6	Slush-type ice.	22
7	Kaimoo melt residual.	25
8	Assumed thermal ice push ridge.	28
9-16	Melt sequence at AINA beach 1975.	30-33
17	Ice rafted sediment	34
18	Beach pitting	36
19	Beach slumping.	37
20	Fan deposit within cusp embayments.	38
21	Dimensions of ice push ridge.	40
22	Ice floe and pushed sediment ridge.	40
23	Cross section of ice push ridge	44

LIST OF SYMBOLS

Symbols from the Roman alphabet

A	average annual rate of sand transport
a_b	wave amplitude at breaking
B_Y	net bottom friction stress on shore in longshore direction
C_f, C_f'	coefficient of friction
c, c_g	wave velocity
D	thickness of the mobile layer of sediment
d, d_b	depth of water
E	wave energy density
g	acceleration due to gravity
H, H_b	wave height
I	immersed weight transport rate
K, K'	coefficient of proportionality
k	hydraulic roughness of beach surface
L, L_o, L_b	wave length
l	distance between rip currents
l_p	length of a plate
m	slope of the beach
P	wave energy flux
P_l	longshore component of wave energy flux
P_{LT}	wave energy lateral thrust
p'	pore space correction factor

S_w	unit volume of sand transport
s	small fraction of energy responsible for setting up longshore currents
T	wave period
U_g	longshore grain transport rate
U_m	maximum horizontal velocity of a water particle
V	longshore current velocity
$W\%$	percent of water that can be held by sand
X_l	beach site length
X_b	foreshore zone width

Symbols from Greek alphabet

α	angle of incidence between wave crest and shoreline
β	coefficient of horizontal mixing
γ	ratio between the breaker height and water depth
δ	a small angle to the normal of the shoreline
η	angle of the slope of the beach
θ	angle of wave crest over specific bottom contour
λ	type of breaking wave
ρ	density of the lake water
ρ	density of the sand
τ	stress per unit area exerted by waves on the water in the surf zone
ϕ	intergranular angle of friction

1. INTRODUCTION

THESIS TOPIC

Sediment transport has been studied extensively on marine and high-energy beaches where both ice action and the effects of wave energy are important. The seasonal cycle of ice influence on beach sediment has been amply described qualitatively from field work on the coasts of the Arctic, Antarctic, and some mid-latitude lakes including the Great Lakes. Sediment transport alongshore by wave action has been described by empirical equations developed from work on the coasts of the Atlantic and Pacific Oceans, the Gulf of Mexico, the North Sea, the Great Lakes, and from laboratory wave tank experiments. Very little work has been done, however, on sediment transport in low-energy environments by ice and wave action. This study encompasses a qualitative and quantitative analysis of sediment movement under ice and wave conditions on a large subarctic lake. Because lacustrine environments experience, on the average, a lower energy flux for both wave and ice conditions than those of marine or Great Lakes environments, the relative importance of factors influencing the rate and amount of sediment movement may be different. These factors include the variables for control of energy flux, grain size of sediment available, the roughness of the bed surface over which the sediment is moving, and the kinematic viscosity of water. The major controlling variables of energy flux under ice conditions include the volume and structure of the ice, the relative amounts of wind energy, and the maximum fetch of ice from its

initial position to its point of contact with the shore. The variables determining the amount of energy flux alongshore by wave action are the wave height at breaking, wave period, angle of incidence of the wave to the shoreline at breaking, submarine or sublacustrine nearshore topography, and longshore current velocity which includes the previous three factors plus considerations of friction from the bed surface and energy dissipation due to turbulence in the mixing zone. The aim of this thesis, then, is to determine the relative influence of these factors in the lower energy regime of Kluane Lake as compared with higher energy environments previously studied. Because of the lower energy present, more precise field measurements could be obtained in two ways. First, the size and degree of sorting of each of the ice push ridges can be more accurately measured and a closer qualitative examination of the volume and structure of the ice can be obtained. Secondly, the greater rate of recovery of marked sediment used in tracing movement alongshore results in more accurate readings of the sediment transport rate without compromising the field environment as in laboratory conditions.

RESEARCH AREA

The study area was part of the shoreline of Kluane Lake in the southwestern Yukon Territory. The lake lies along a fault zone in a valley known as the Shakwak Trench which is bounded by a range of the St. Elias Mountains on its western side and a lower range of mountains, the Kluane Hills, on its eastern side (Figure 1). The lake, the largest in the Yukon, measuring approximately 70 km in length and varying between

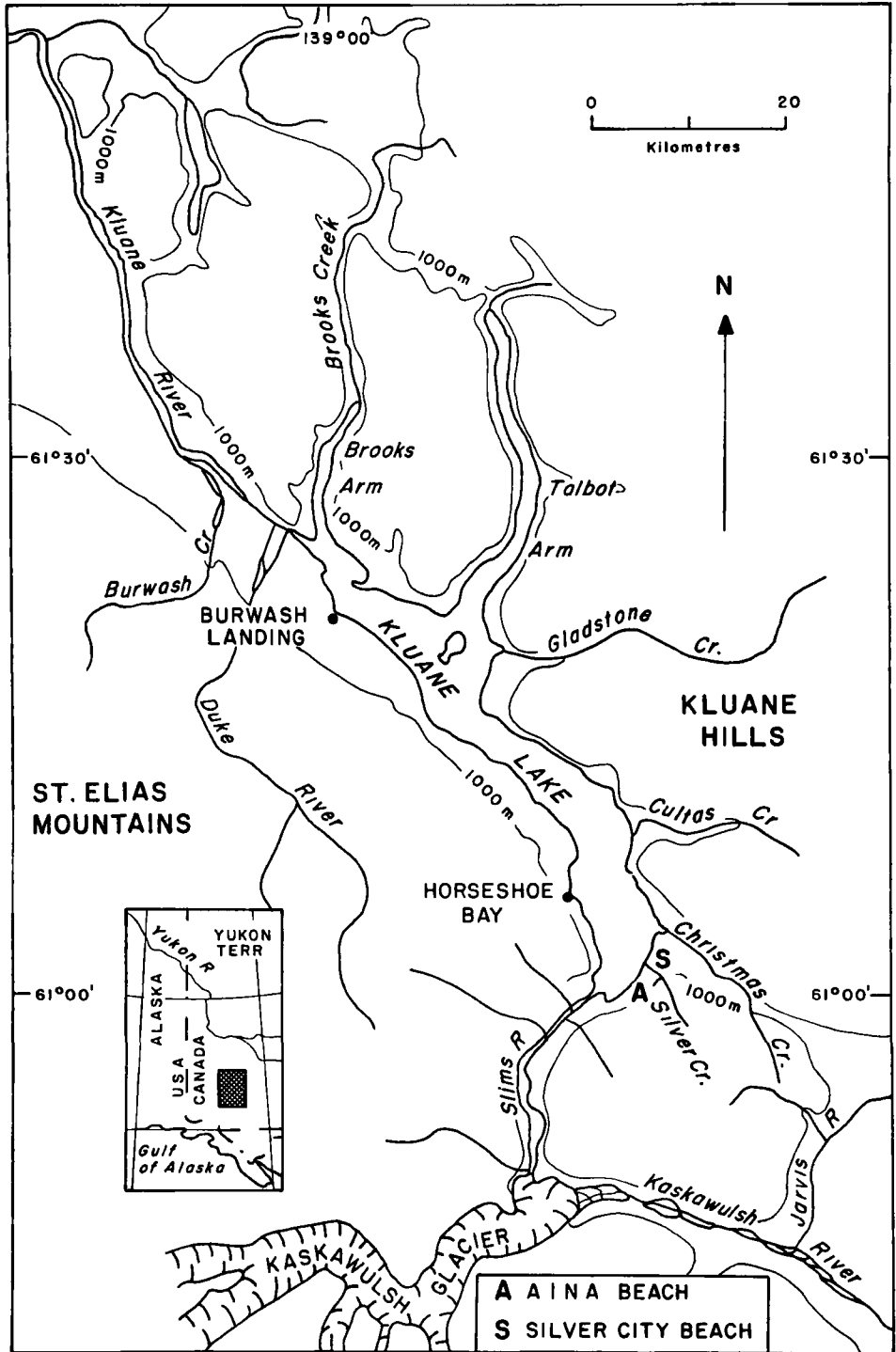


FIGURE I: KLUANE LAKE, YUKON TERRITORY
 (after Bostock, 1969.)

5 and 15 km in width, lies in a north-south orientation. There are many influents on either side of the lake, but the major one is the glacially fed Slims River flowing north from the Kaskawulsh Glacier and entering Kluane Lake at its southernmost end. Its discharge, usually very low from October to April, increases during the summer and peaks around the first week in August. This causes a general rise in the lake level through the summer months. For example, lake water level readings taken at Horseshoe Bay, on the southwestern shore of the lake, by the Water Survey Branch of the Department of Environment from May 16 to August 1, 1975 show it rising 1.6 vertical m. Kluane Lake has only one effluent, the Kluane River, located in its northwestern corner just south of Brooks Arm. Aerial photographs of the lake taken in August of 1972 and field reconnaissance during the summer of 1974 indicate that its coastline is quite varied, ranging from broad beaches of primarily alluvial sediments, to drowned estuaries, to cliffs. Most of the beach material is derived from the glacial sediments of the Shawak Trench.

LITERATURE SURVEY

Much descriptive work has been done on the seasonal cycle of ice formation and decay and its effect on beach sediment. In formation, the development of ice slabs and kaimoo has been defined by McCann and Carlisle (1972) and discussed in articles by Rex (1954), Moore (1966), Davis (1973), and Marsh, Marsh, and Dozier (1973), and other minor features formed at this time are described by Greene (1970), and Dionne and Laverdière (1972). There have been observations and some calculations on the effect of lake

ice on sediment which explain the mechanisms of thermal expansion and contraction and periodic fluctuations of the lake water level during total ice cover (Scott, 1927; Wilson, Zumberge, and Marshall, 1954; Sundberg-Falkenmark, 1957; and Wagner, 1970). During breakup, descriptions of ice-rafted and ice-pushed detritus have been recorded by Rex (1955), Dionne (1969), Bryan and Marcus (1972), Hume and Schalk (1964, 1973), and Davis (1973). Except for thermal contraction and expansion during total ice cover and the microrelief features of ice breakup and melt, most of these studies dealt with high-energy marine and Great Lakes environments. Since this thesis is concerned with lower energy environments, greater attention is paid to the size, sorting, and other details of different disturbances of sediment caused by ice. A more complete literature review is included in the chapter dealing with ice.

Work on sediment transport in open-water energy conditions has been both qualitative and quantitative. Articles which laid the foundations of detailing this process both descriptively and empirically include studies by Putnam, Munk, and Traylor (1949), Johnson (1956), Kidson and Carr (1959), Inman and Bagnold (1963) and Ingle (1966). From the pioneer work by Putnam, Munk, and Traylor (1949), work on developing empirical equations for longshore current velocity has proceeded (Caldwell, 1956; Galvin, 1967; Longuet-Higgins, 1970, 1972) by accounting for many more variables such as mixing length, radiation stress, and the utilization of a more sophisticated approach in defining the coefficient of friction. Expanding upon Inman and Bagnold's (1963) equation for the rate of alongshore sediment transport were Komar (1969, 1971), Komar and Inman (1970), De Vries (1971), Battjes (1975) and Motyka and Willis (1975). As in the

case of ice, a more complete literature review is included in the chapters discussing the mechanics of sediment transport under wave energy conditions.

CLIMATE AND GEOMORPHOLOGY OF STUDY AREA

The climate of the region around Kluane Lake is typically sub-arctic and semiarid. Yearly average values for temperature and precipitation in the Whitehorse area, approximately 290 km east southeast of Kluane Lake, include mean annual maximum temperatures of 4.1°C and mean annual minimums of -5.8°C taken over a period from 1942-1970, and a mean total precipitation of 260.3 mm per year during the same 28 year period (Hare and Thomas, 1974). Climatic data for the summer months at Kluane Lake were recorded by Traylor Barge (1969) from May to August during the years 1963-1965. She recorded an average summer temperature of 50°F (10°C) with a daily range of 20°F (11.1°C), and an average daily precipitation of 0.9 mm with a 34 percent probability of rain in any one day. She also found the winds to be generally light, averaging around 4 knots, predominantly from the south and east at night and southeast during the day. During the 1974 and 1975 summer field seasons, the winds were observed to be predominantly stronger in June and August, averaging 6.5 m/hr (10.5 km/hr), than in July where, although the average 6.02 m/hr (9.7 km/hr) was not much less, the winds were much more variable. Also during these field seasons, the wind direction in July was predominantly from the southeast and in August from the north. It is from the northern end of the lake where the waves affecting southern beaches have the greatest fetch and more closely approximate higher energy environments.

There has been little major geomorphological research in the Kluane Lake region. Bostock, from a field reconnaissance in 1952 and in a later article (1969), hypothesized a chronology of development for the lake, taking account research reports on glacial chronology (Denton and Stuiver, 1966), the Slims River morphology (Fahnestock, 1969), and the general geology of the area (Muller, 1967). From this chronology, a better understanding of the varied coastline can be attained. According to Bostock (1969), when the Ruby Ice Sheet, which occupied the Shawkak Trench, began to melt between 50,000 and 25,000 B.P., it drained first through the Burwash Valley System, then down the Slims-Kaskawulsh System after the Kaskawulsh Glaciation about 12,500 B.P. . This drainage pattern continued throughout the post-glacial period, and the lake began to take form. Around 2,500 B.P. a Neoglacial advance occurred involving the alpine valleys of the St. Elias Mountains and reached a maximum about 400 B.P.. At this time, the Kaskawulsh advanced so far that the Slims River was cut off from the Kaskawulsh River and reversed its flow northward towards the lake. Because of this, the lake water level rapidly rose from 40 ft (12.2 m) below, to 30 ft (9.1 m) above, its present level. Accompanying this rise in level, the Kluane River system grew as an outlet and eventually cut its channel to bedrock where it now maintains its discharge and the lake level. Because of these fluctuations, both drowned estuaries and raised beaches can be found along the coastline of Kluane Lake.

The other major piece of geomorphological research of the lake was undertaken by Bryan (1971) in which he studied the different forms of sedimentation around and in this glacially fed lake. He concluded that there were three major processes affecting sediment distribution which were:

eolian, density currents, and ice and wave action. The eolian process occurred with the down valley winds stirring up the loess on the Slims River Delta. A more in-depth study of this phenomenon has been done by Nickling (1975). Offshore sedimentation by density currents was the major concern of Bryan's (1971) work. He reasoned, from offshore bottom cores and bathymetric surveys, that sediment was deposited by the Slims River through the action of the colder sediment laden river flowing under the lake water in the form of a current until the sublacustrine topography slowed it down. Ice and wave action were the processes, as discussed by Bryan (1971), which affected the sediment of the coastal and nearshore areas, causing push ridges and rafting of detritus by ice and alongshore movement of sediment by wave action. The present study attempts to take a more detailed view of this third process.

SITE DESCRIPTION AND METHODOLOGY

Two sites were selected for measurement during the 1974 field season on the basis of location, which facilitated daily observation, and differences in composition and form. The same two sites were used in 1975. The first site was located at the Arctic Institute Base Camp (referred to as the AINA beach) on the southeastern shore of Kluane Lake (Figure 1). This site is situated on part of an alluvial fan which forms about 5 km of the shoreline of the lake (Plate 1). The second site was located 2.4 km from the AINA beach just north of Silver Creek and Silver City (referred to as Silver City beach) in front of a 30 to 60 m cliff (Figure 1) (Plate 2).

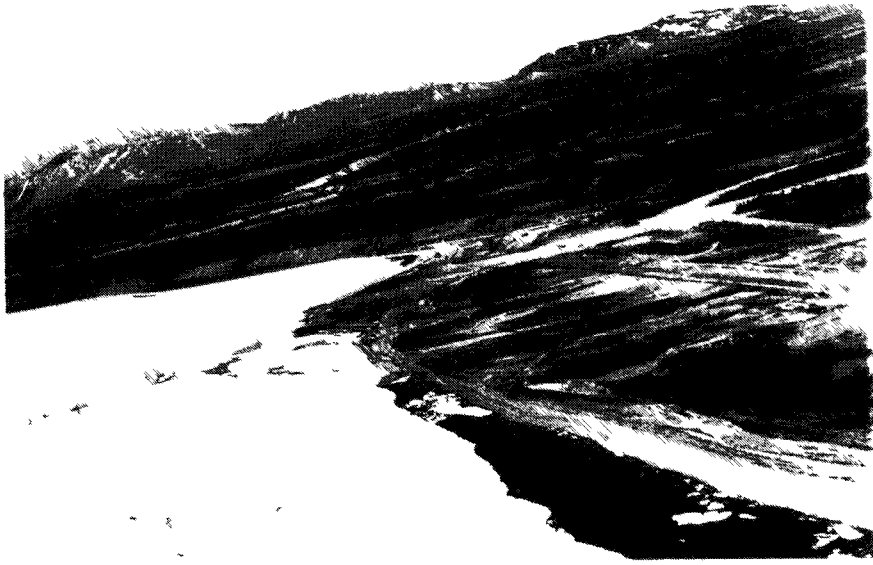


PLATE I: AINA beach site



PLATE 2: Silver City beach site



PLATE 3: Silver City beach sediment

Beach and sediment characteristics were determined through profiling, sampling and observation. A grid of 5 lines 8 m apart was laid out for profiling the beach and collecting the sediment samples. Profiles were measured once a week by a surveyor's level with a one degree accuracy from May 26 to August 6 through the 1975 field season. From figures 2 and 3, the AINA beach is depicted as a broad, shallow beach and the Silver City site is narrow and steep. The greatest change in the profiles, over time, that is evident on both these sites is the dramatic rise in the lake level. This rise is accompanied by a gradual build up of sediment within the foreshore zone of both beaches although this is much less evident at Silver City. At the AINA beach site, 5 sediment samples were taken along each profile at 2 m intervals starting from the waterline. Apart from the one set of samples midway down the lines, which was composed of moderately sorted medium sized sand grains, the sediment was coarse sand and poorly sorted (Table 1). The same procedure was employed at the Silver City beach site where a mean sediment size of medium gravel occurred which was moderately to poorly sorted (Table 2). At Silver City beach, a number of small boulders were not recorded in this statistical survey because of logistical problems of measurement. (Plate 3).

From this descriptive account of each beach site, some inference can be drawn as to the origin of the sediment and the amount of energy currently present. The AINA beach reflects its alluvial origins from the presence of the poorly sorted coarse sand. Evidence from three descriptions of this beach indicate a low energy regime. First, only the set of sorting values for the samples in row 3 in Table 1 indicate that even a moderate amount of sorting has taken place whereas there is generally poor sorting on either site of this row. Second, through the summer there is a gradual

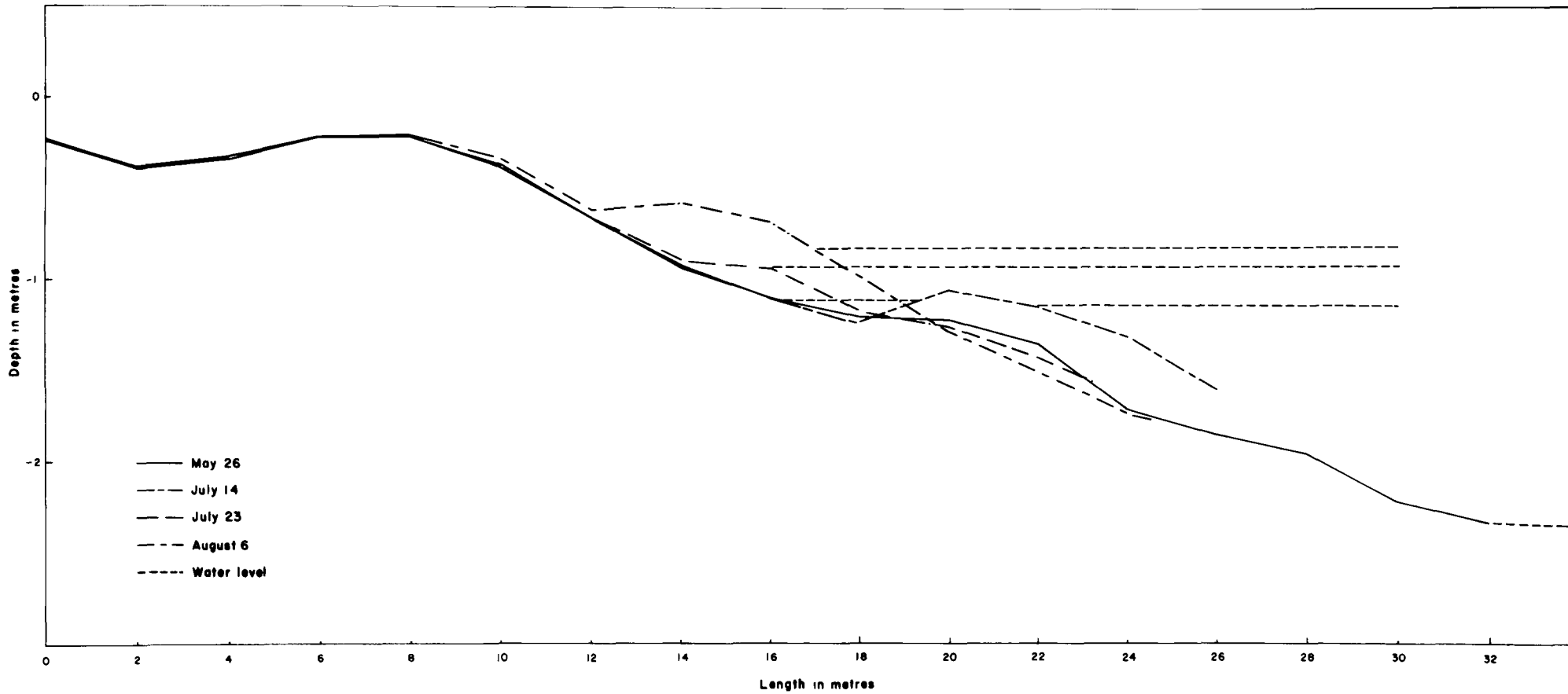


FIGURE 2 A I.N.A. BEACH PROFILE

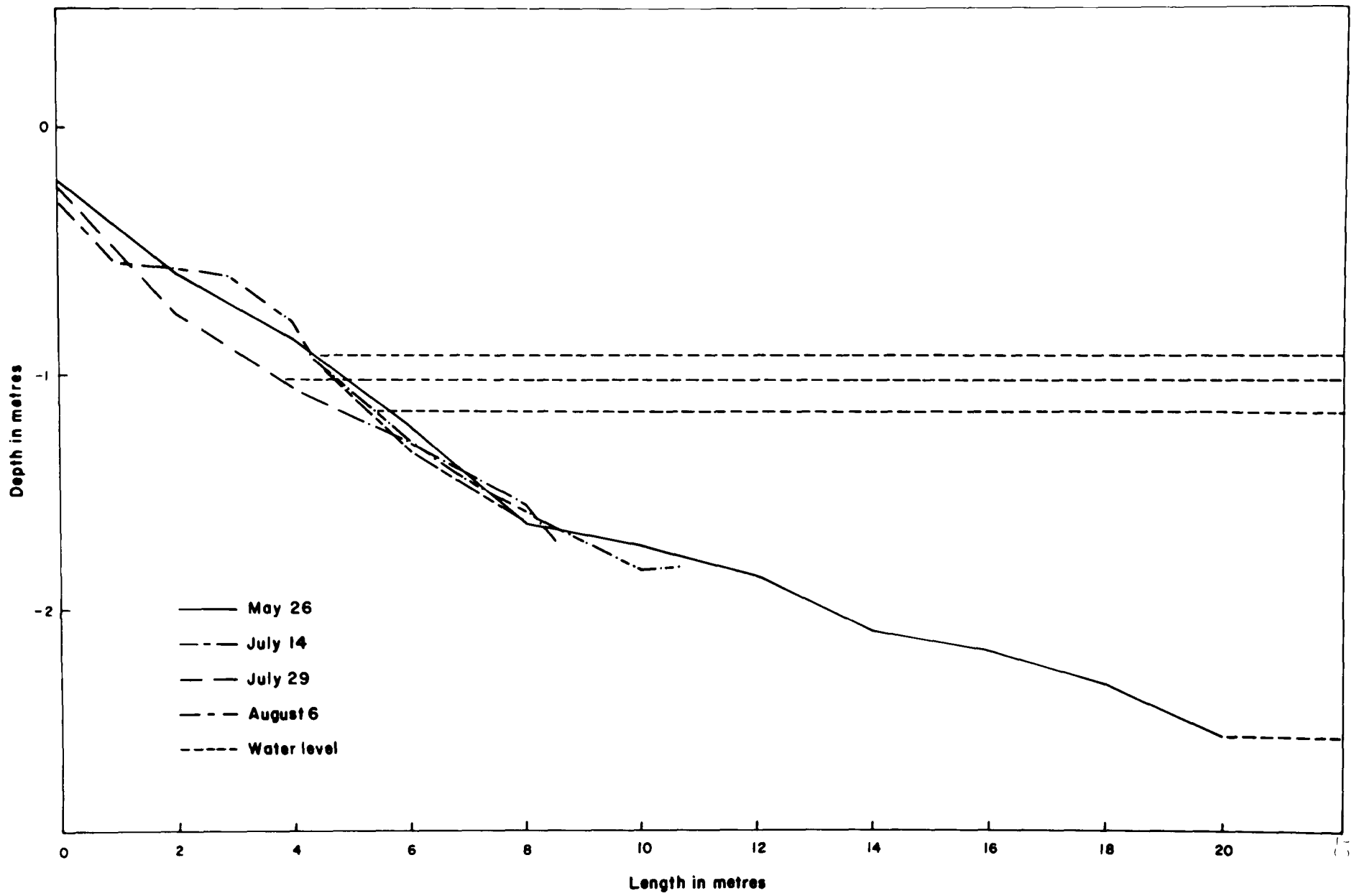


FIGURE 3: SILVER CITY BEACH PROFILE

TABLE 1

AINA beach sediment sorting characteristics

Profile lines		A	B	C	D	E
Rows						
1	\bar{X}	-0.70	-0.52	-0.60	-0.48	-0.10
	σ	1.49	1.32	-	1.83	1.80
	v	poor	poor	-	poor	poor
2	\bar{X}	-1.15	-0.03	-0.50	-0.82	0.83
	σ	1.80	1.45	0.36	1.90	1.26
	v	poor	poor	well	poor	poor
3	\bar{X}	0.73	1.03	0.70	1.37	1.12
	σ	0.97	0.89	0.82	0.48	0.52
	v	moderate	moderate	moderate	well	moderate
4	\bar{X}	-0.70	-0.60	-0.48	0.82	0.82
	σ	1.79	1.80	-	1.10	-
	v	poor	poor	-	poor	-
5	\bar{X}	-0.33	0.40	-1.15	0.57	0.12
	σ	1.50	1.04	1.73	-	0.98
	v	poor	poor	poor	-	moderate

(\bar{X} , mean is phi size units; σ , standard deviation; v, the verbal statement on sorting)

TABLE 2

Silver City beach sediment sorting characteristics

Profile lines		A	B	C	D	E
Rows						
1	\bar{X}	-3.5	-3.95	-3.98	-5.00	-4.57
	σ	2.10	1.28	1.50	0.57	1.26
	v	very poor	poor	poor	moderately well	poor
2	\bar{X}	-	-5.20	-4.53	-4.73	-3.77
	σ	-	0.04	.95	0.79	1.91
	v		very well	moderate	moderate	poor
3	\bar{X}	-3.90	-3.83	-4.57	-4.43	-3.45
	σ	1.75	-	1.45	0.91	1.99
	v	poor	-	poor	moderate	poor
4	\bar{X}	-4.97	-4.13	-3.63	-4.17	-4.2
	σ	0.70	1.52	0.85	1.53	-
	v	moderate	poor	moderate	poor	-
5	\bar{X}	-4.47	-4.6	-5.00	-3.47	-2.75
	σ	1.29	1.21	0.65	1.96	2.18
	v	poor	poor	moderately well	poor	very poor

(\bar{X} , mean in phi size units; σ , standard deviation; v, verbal statement on sorting)

accretion of sand while the lake water level rises which is indicative of a low-energy regime. Third, although the beach material is poorly sorted, the surficial sediment has a regular pattern of fine to coarse sand in stripes parallel to the shoreline, which again is indicative of low-energy environments. The origin of sediment on the Silver City site would likely be from 30 to 60 m cliff composed of glacial till located just behind the beach. When the lake level was higher, erosion of the cliff took place depositing sediment on the beach. Through wave action, the smaller material was winnowed out leaving a narrow, steep gravel beach. From the change in profiles (Figure 3) and the degree of sediment sorting (Table 2) this beach can also be assumed to be affected by a low amount of energy.

During breakup daily observations of movement of the lake ice were taken at both sites. However, when the study focused on sediment movement under wave energy conditions, the Silver City site was dropped because the layer of small boulders at the shoreline inhibited any movement of the 9, 4, and 2 mm sand grains that were being used for testing. The larger indigenous sediment did not move either because the energy was too low. Therefore it was concluded that this site was static during the majority of the season with respect to the longshore movement of sediment by water waves, and was not suitable for testing.

2. SEDIMENT DISTURBANCE BY LAKE ICE

Kluane Lake is affected by ice for approximately 8 months of the year, commencing with formation in October and terminating with breakup in late May or early June. Because the lake is dominated by ice for two-thirds of the year, Bryan (1970) postulated that the ice would have a considerable effect on the coastal sediments of the lake. To test this hypothesis, a field observation program during ice breakup was established in May, 1975. This program was based entirely on observation and accepted descriptive measurement techniques and because of the lack of facilities for measurement of various factors, no model construction was attempted to predict the development of ice push ridges and other breakup phenomena. The program consisted of daily observation, which included photographing each site from a tower erected at the AINA beach and the cliff located behind the Silver City beach, recording the relative position and condition of the ice with respect to each beach site, and weekly profiling using the grids previously described. When ice push of sediments occurred on the beach, the dimensions of both the sediment and ice floe involved were measured, and samples of the ridge were analysed to determine the difference in sorting between it and the undisturbed beach sediment. Observations were also made in the vicinity of the two sites to record any other types of breakup phenomena occurring at this time.

An understanding of the type of ice present on the lake is crucial to the evaluation of the effect it will have on the sediment of the beaches. The description and classification of various types of ice have been amply

presented by Wilson et al (1954) (Figure 4) and the relative strengths of these types were determined by Butkovich (1955). According to figure 4, three major ice types, sheet ice, slush agglomerate ice sheet, and floe and pan agglomerate ice sheet are depicted as the final stages of ice development during formation. Although this figure shows the sequence of formation of ice types, it has been observed that the reverse may occur during breakup. All three types of ice probably existed during the season, but only sheet ice, which had broken into floes, and slush ice, a highly deteriorated form of sheet ice, existed during breakup on Kluane Lake in the 1975 field season. Sheet ice (Plate 4), characterized by a smooth unbroken surface, is formed under reasonably calm uniform conditions where heat loss is only through upward conduction. It is composed of a columnar aggregate of crystals with c-axes vertical (Wilson, et al, 1954) (Plate 5). Because this ice is composed of large crystals, with small length-to-width ratios, it has a high crushing strength (Butkovich, 1955). This ice, either in sheet or floe form, was dominant on the lake from the start of the field season, May 19, to the last week of May. During this period, the ice broke into floes and became increasingly more fragile with its crystal aggregates breaking into small pieces known as candle ice. The ambient daytime air temperature throughout this period ranged from a high of 14°C to a low of 0°C . Through the first half of this period, when the daytime temperatures were 7°C to 10°C and the nightly minimums frequently fell below freezing, there was a freeze-thaw sequence on the lake which resulted in the formation of a quasi floe-agglomerate ice sheet type. Wilson (1954) described this ice sheet as characterized by marked variations in thickness and texture and having a rough heterogeneous cover. However, because most of the ice was

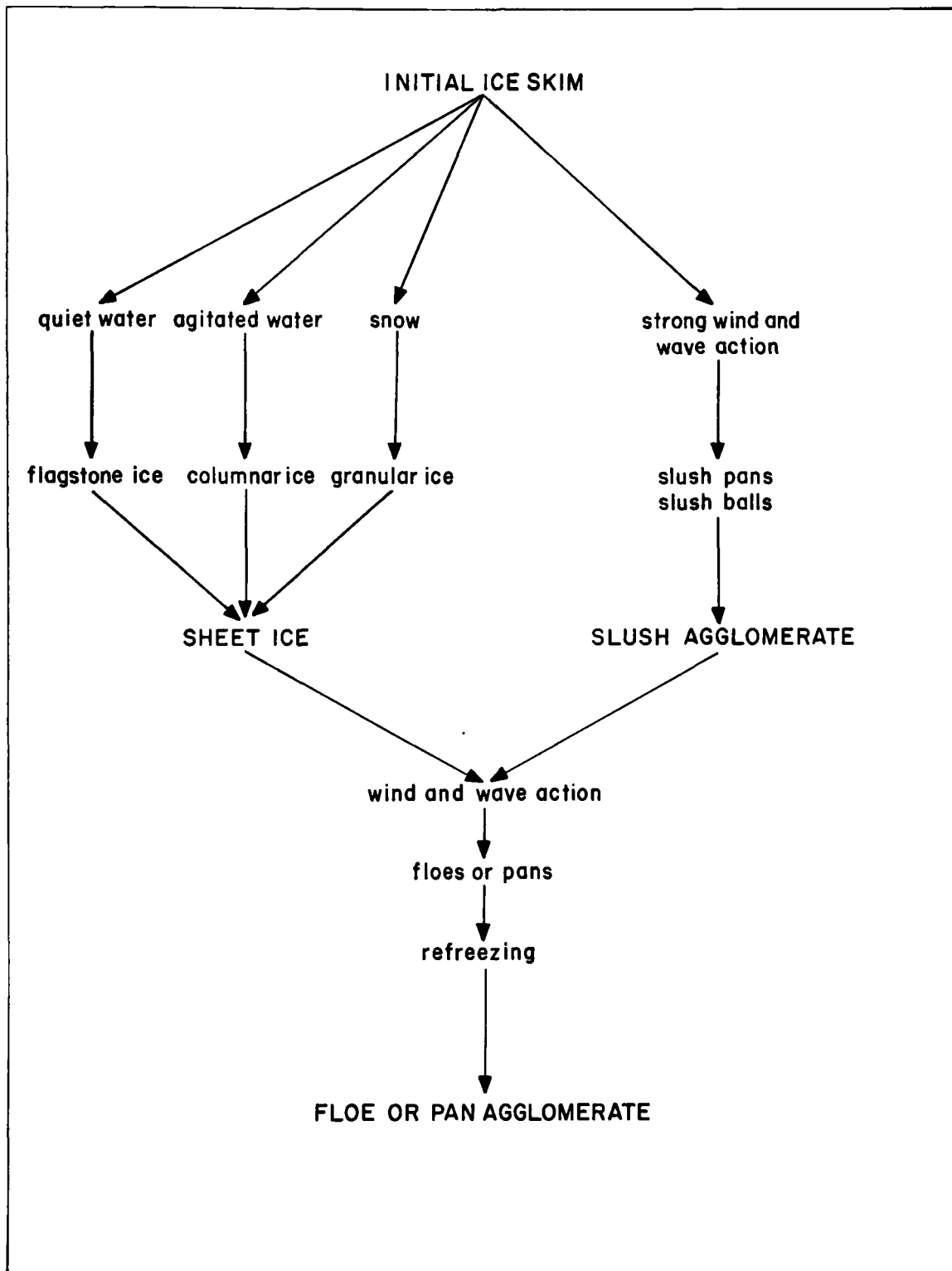


FIGURE 4. CLASSIFICATION AND DESCRIPTION OF ICE-COVER IN FORMATION (after Wilson et al, 1954.)

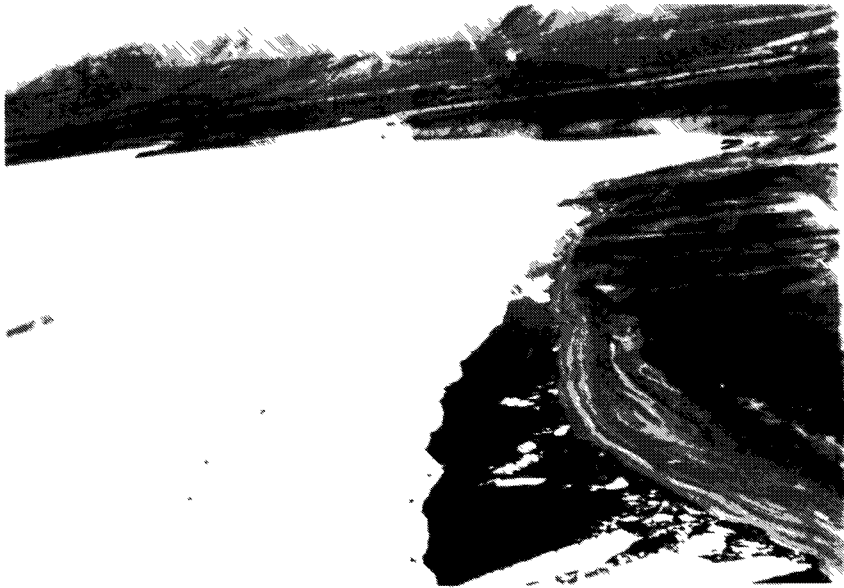


PLATE 4: Sheet ice floes



PLATE 5: Sheet ice crystals

sheet ice in a state of either ice floes or refrozen ice floes and did not have marked variations in thickness or texture, the ice of Kluane Lake could more accurately be described as a temporary sheet ice floe-agglomerate. Later in the field season, towards the **first** week in June, the minimum temperatures averaged 6°C and winds of 16 to 24 km per hour occurred breaking the sheet ice into floes of slush ice (Plate 6). This type of ice has an irregular lumpy surface composed of condensed frazil (Wilson, et al, 1954) which in this case is a deteriorated form of sheet ice. According to Butkovich (1955), this type of ice would be relatively weak because of its frazil, small grained crystal, composition. From these observations of ice types during breakup at Kluane Lake, a corresponding flow diagram was made (Figure 5) to complement the one developed by Wilson, et al, (1954) (Figure 4).

Ice affects the beach sediment during formation, total cover, and breakup, constituting a seasonal cycle. During formation, sediment is generally included within the ice and the different ice forms which are created. Rex (1964) and Davis (1973) stated that the first features that are formed during this period are ice slabs. They occur when the autumn storms produce a spray from the waves which falls on the subfreezing surface of the beach and freezes on contact, cementing the sediment lying within this area of the beach. With continued cold and wave activity, a kaimoo or ice foot develops. McCann and Carlisle (1972) defined a kaimoo as strictly the result of freezing of swash in a microtidal or non-tidal environment built up above the still water level and usually containing interbedded sediment derived from the water covered beach below. They differentiated the kaimoo from the icefoot by defining the icefoot as developed in the upper part of the intertidal zone of tidal beaches, located within a zone from considerably above to well below



PLATE 6 : Slush-type ice

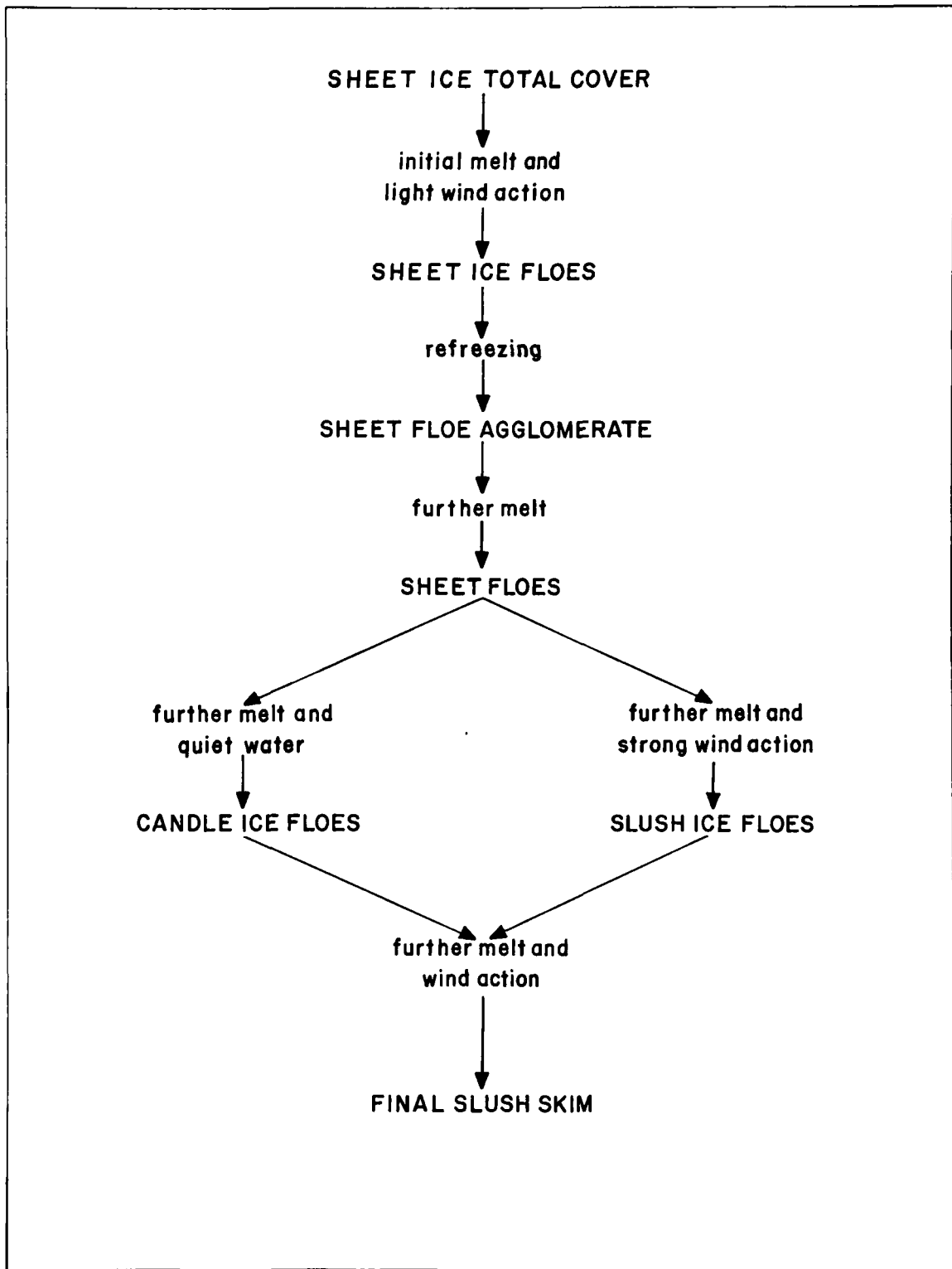


FIGURE 5. CLASSIFICATION AND DESCRIPTION OF ICE-COVER DURING BREAKUP AND MELT AT KLUANE LAKE.

the high water level. Also, no interbedding of sediment is apparent within the icefoot. Since Kluane Lake experiences no tides, a kaimoo and not an icefoot is developed during this period. Marsh, et al, (1973) reported that the conditions for kaimoo development in lacustrine environments include subfreezing air temperatures with an open lake containing a supply of ice fragments. Once these conditions are met, the freezing of swash spray and interbedding of sediment commence. They also stressed that the ridge which develops as a result of this process rarely attains a height of over one meter. Although the 1975 field season commenced after most of the beach fast ice had melted, evidence of interbedding of coarse and fine sediments were apparent from wave cut sections developed during occasional mid-to-late summer storm (Plate 7). Other ice-sediment features formed at this time that have been widely recorded are ice contact cusps, slush balls and ice cakes. Ice contact cusps, according to Dionne and Laverdière (1972) are formed by waves eroding the shoreward edge of the kaimoo into rounded promontories separated by narrow embayments, freezing and remaining in situ until breakup. The existence of ice cakes has been recorded by Rex (1964), Greene (1970), and Dionne and Laverdière (1972) and have been described as a block of ice with an interbedding of sediment caused by its unusual process of formation which consists of alternating floating and freezing on the beach surface over a certain length of time. Many of these ice cakes are often thrown far up on the beach where they rest until spring melt. Slush balls are formed on the lakeward edge of the kaimoo by a rolling action of frazil ice in storm waves and have been observed by Wilson, et al, (1954) and Davis (1973). Within these balls lies a coil of sediment added during the process of formation by suspended sediment freezing to the ball. Each of

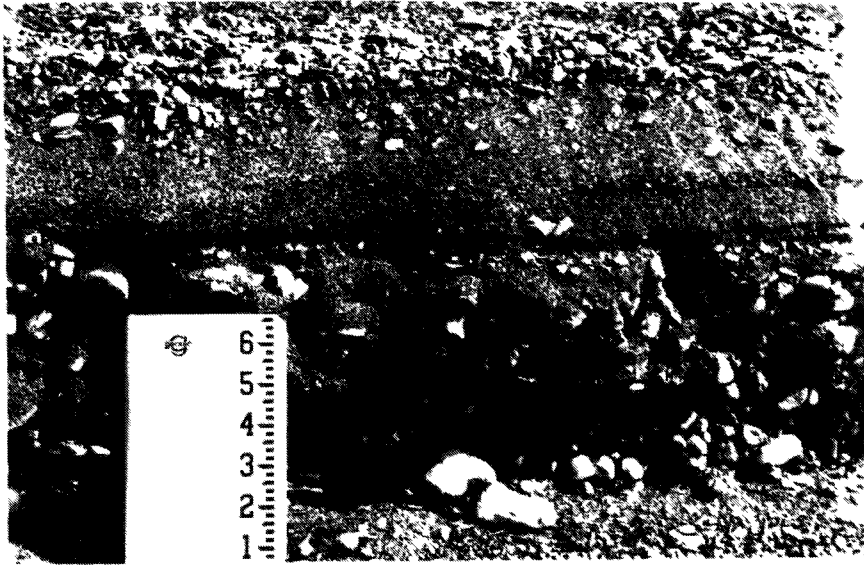


PLATE 7: Kaimoo melt residual

these features may have been formed at Kluane Lake, but none were observed in their original state in 1975 because breakup was underway when the field season began. However, evidence of their existence in the form of melt features was observed.

Total ice cover, which exists on Kluane Lake from approximately late November to mid April, is a dormant period in the action of ice on beach sediments. The predominant type of movement during this period is the mechanism of thermal expansion and contraction of ice. The underlying principle of this phenomenon is that ice expands when warmed and contracts when cooled. The sequence of events is as follows. A rapid fall in nighttime temperatures causes the lake ice to contract and form tension cracks. These cracks are then filled with water which immediately freezes. With a subsequent rise in temperature, the ice expands. However, because of the added area caused by the infilled tension cracks, the ice sheet is larger than the lake and therefore may cause push of the beach sediment into ridges (Wilson, et al, 1954). Wilson, et al, also reported that on Wamper's Lake, a temperature rise of 0.56°C per hour prolonged over a 12 hour period on a 20 cm ice sheet was sufficient to cause visible thrust on a shore composed of unconsolidated glacial outwash containing some boulders. They further pointed out that, from developing theoretical equations relating ice thickness and temperature change to the maximum ice push that could occur, the relationship between temperature rise and maximum push is not linear because the sheet would be confined at the shore and because of the factor of the plasticity of ice. The 1975 field season began after most of the ice was melted from the shore so that a comparative study with Wamper's Lake could not be accomplished. However, a ridge of sediment was observed that had the characteristics of

being a thermally produced ice push ridge. It was located in a small embayment just south of the Silver Creek delta approximately 6 m inland and running parallel to shore. The sediment on the side towards the shoreline also looked as if it had been moved whereas the sediment on the other side was undisturbed. It was, however, a relatively minor feature (Plate 8). Other minor factors of sediment disturbance by ice during total cover that have been reported include Sundberg-Falkenmark's (1957) study of push caused by ice expansion due to rising and falling water levels, and a study by Rex (1955) which looked at the effect of grounding of sea ice causing microrelief features offshore. Because the water level of Kluane Lake is directly related to the melt water inflow from the Kaskawulsh Glacier, which in turn is directly related to climatic conditions, the ice and shore sediments would not be affected by a rise and fall of the water level during the period of total cover. Although offshore gouging of ice does exist, the amount of permanent alteration to the beachface is deemed negligible.

From the middle of April to the first week of May, breakup began at Kluane Lake with the melt of the kaimoo and beachfast ice from the shore. By mid-May, when the 1975 field season began, the beach was relatively free from ice but the lake was almost completely covered, with only .5 to 1 m of open water occurring at the shoreline (Plate 9). The ice continued to deteriorate through May to the first week of June. In accordance with meteorological data of temperature and wind direction and velocity, as previously mentioned, a sequence of deterioration developed. With the formation of puddles on the ice closest to shore, the ice started to crack when certain portions had been sufficiently weakened by melt. After this,

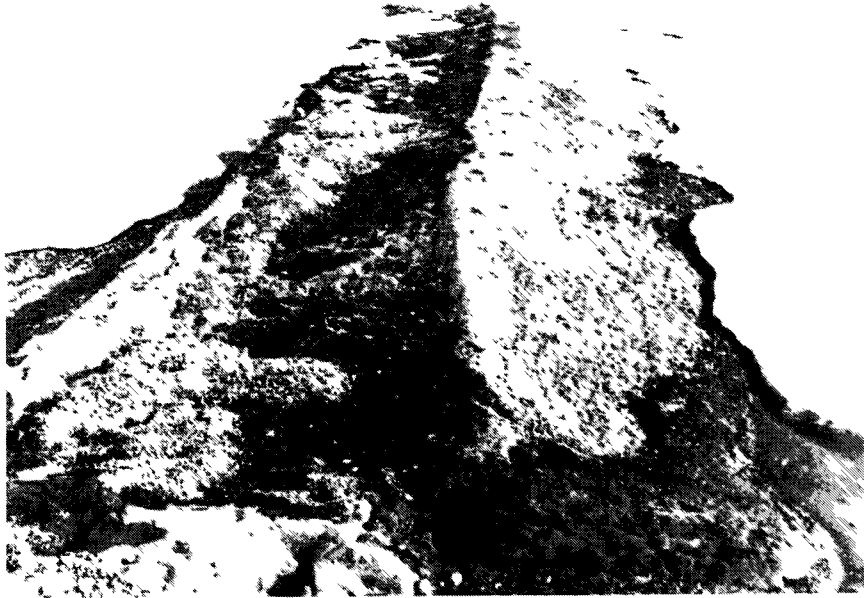


PLATE 8 : Assumed thermal ice push ridge

the ice farther from shore began to form puddles and crack into floes. This pattern continued with the wind blowing the ice both towards and away from the shore until June 2nd. On this day a strong wind from the Slims River valley southeast of the beach sites broke the remaining ice into slush and blew it northward. By June 6th, both the AINA and Silver City beaches were clear of ice. The following sequence of plates 9 through 16 depicts this process of deterioration at the AINA beach site.

Melt features that were observed on Kluane Lake beaches during the 1975 spring ice breakup and melt included ice rafted sediment, beach pits or kettle holes, and the remains of an ice-contact cusp type form. Although no erratic boulders were evident in the vicinity of the two sites, as classic evidence of ice rafting as described by Nichols (1961) and Dionne and Laverdière (1972), some ice rafted sediment was observed at this time. However, the rafted sediment that was observed on Kluane Lake appeared to be derived from the local environment (Plate 17). This phenomenon could be explained by a floating ice block which had been grounded during total cover as either part of an ice ridge, described by Davis (1973) as large slabs of ice wedged together and anchored on an offshore bar, or grounded ice, as explained by Rex (1955), and had come loose and floated during the course of breakup. Because the majority of the ice rafted sediment observed was located near the Silver Creek delta, it was assumed that the detritus was derived from an offshore bar. Pits and kettle holes have been observed and described by several authors. Nichols (1961), Greene (1970), Dionne and Laverdière (1972), Davis (1973) and Short and Wiseman (1975) all define this phenomenon as a function of melting of buried ice blocks, usually in the form of slush balls or ice cakes that had been transported to the upper part of the

Melt Sequence - AINA Beach 1975



PLATE 9: May 19



PLATE 10: May 25



PLATE II: May 29



PLATE I2: May 31



PLATE 13: June 1



PLATE 14: June 2 8:30



PLATE 15: June 2 16:20



PLATE 16: June 4



PLATE 17: Ice rafted sediment

beach by the autumn storms which occur during freezeup. Evidence that this type of melt occurred on Kluane Lake beaches was found on only one section of the 2.4 km of coastline observed at this time. This section was also near the Silver Creek delta, lending speculation that this area may be a high energy zone for wave attack due to refraction of the waves around the delta. The process of pitting was initiated with the collapse of surficial coarse sand and small pebble layer of sediment, followed by a bubbling action of water percolating upwards carrying with it fine-to-medium sized sand grains (Plate 18). These pits kept widening and percolating for about two weeks. The action, as it occurred on Kluane Lake, was initiated by the melt of an ice block, and probably perpetuated by the melt of ground ice in the general area. At the end of the breakup season, this portion of the beach had slumped so that it was partially inundated with water (Plate 19). The third melt feature, ice-contact cusps, defined previously, were located in the vicinity of the other features near the delta of Silver Creek. These forms appear to have been developed differently from the description postulated by Dionne and Laverdière (1972). They described this feature as having a steep front facing landward and a shallow backslope towards the shoreline. The forms at Kluane Lake, however, were facing in the opposite direction with a steepfront facing the shoreline and a gentle slope landwards. In addition, fans composed of well sorted medium sized sand were located within the embayments of the cusps (Plate 20). One explanation for this phenomenon could be attributed to the conditions during the development of the cusps. The kaimoo was formed during a storm period when cusps existed on the beach. The kaimoo filled in the embayments conforming to the beach form and as it grew the

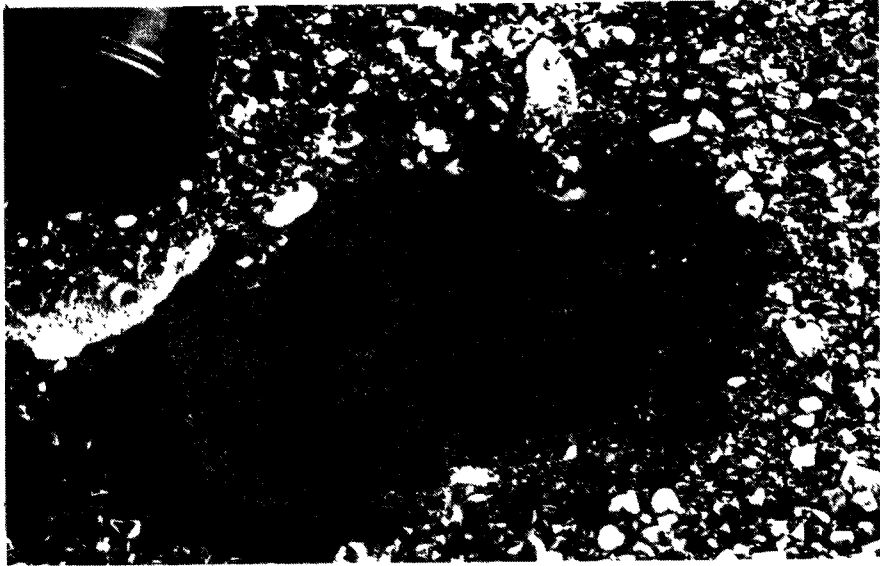


PLATE 18 : Beach pitting

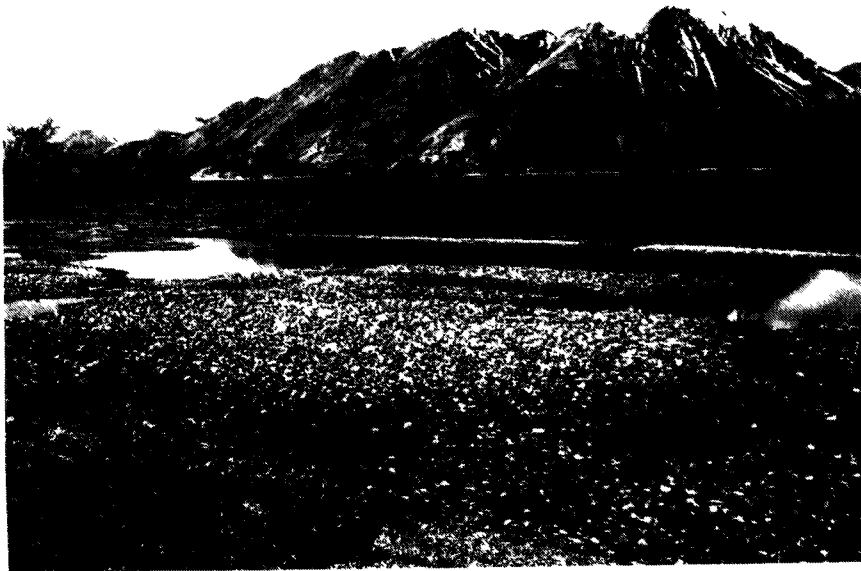


PLATE 19 : Beach slumping

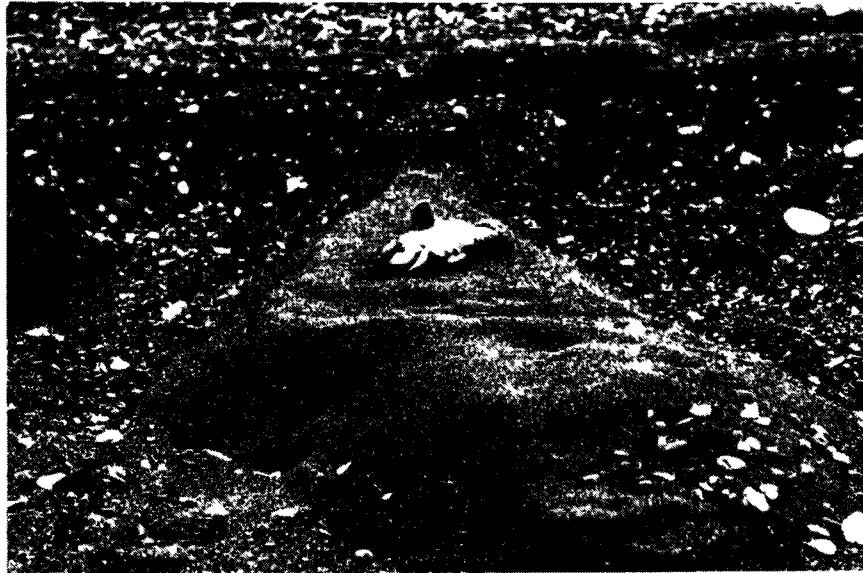


PLATE 20: Fan deposit within cusp embayments

landward edge built up sediment in front of it. Finer sediment could have been deposited in the quieter waters between the ice and the beachface. This feature was frozen until spring. Upon melting of the kaimoo, the deposit of finer sediment flowed down the steep shoreward side of the cusp fanning out in the same manner as an aluvial fan. Since freezeup and initial melt were not observed, this description remains merely a conjecture.

The feature most often identified in the literature on ice breakup are ridges caused by ice floes pushing into the beach by the force of wind or other ice masses on the lake (Scott, 1927; Nichols, 1953; Doeglas, 1955; Goldthwait, 1957; Jennings, 1958; Rex, 1964; Moore, 1966; Greene, 1970; Wagner, 1970). This ice floe acts as a miniature glacier pushing debris in front of it as an end moraine and striating the beach sediments underneath (Dionne, 1972; Hume and Schalk, 1973). Hume and Schalk (1973) report that on marine beaches around Point Barrow, Alaska, this action of sediment disturbance generally accounts to 1 to 2 percent of the total volume of beach sediment lying above sea level, but can, in some cases, account for up to 10 percent of the total volume. In one such case, an ice push mound was measured to be over 2 m high, over 50 m long and was located as much as 100 m inland from the ocean. Ice push ridges did not occur on Kluane Lake until the ice sheet began to break into small floes. Therefore, period of push was confined to a little less than one week beginning May 28 and lasting until June 1 after which only slush ice prevailed. The dimensions of the four ice push ridges and their corresponding ice floes were measured during this period (Plate 21 and 22) (Table 3), and sediment samples from two ridges on the AINA beach were acquired and analysed for sorting characteristics (Table 4). These sorting characteristics were similar to those of

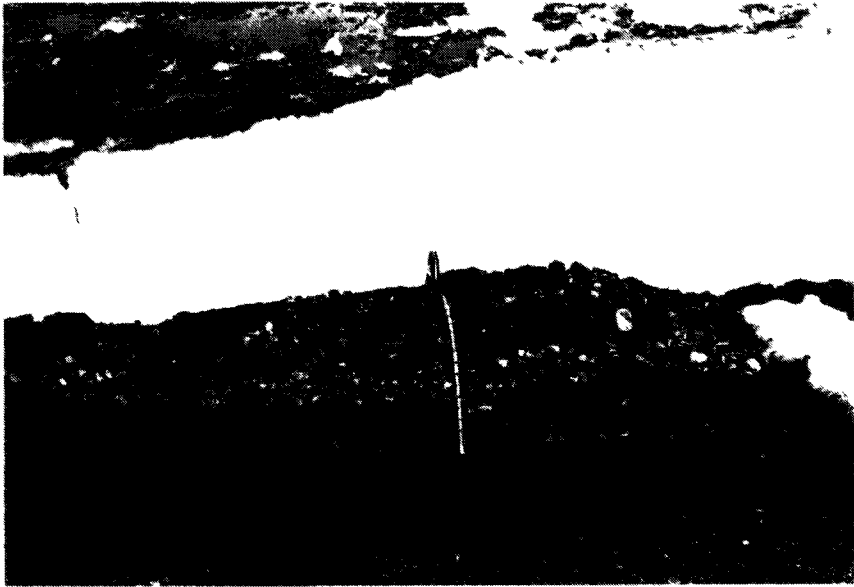


PLATE 21: Dimensions of ice push ridge

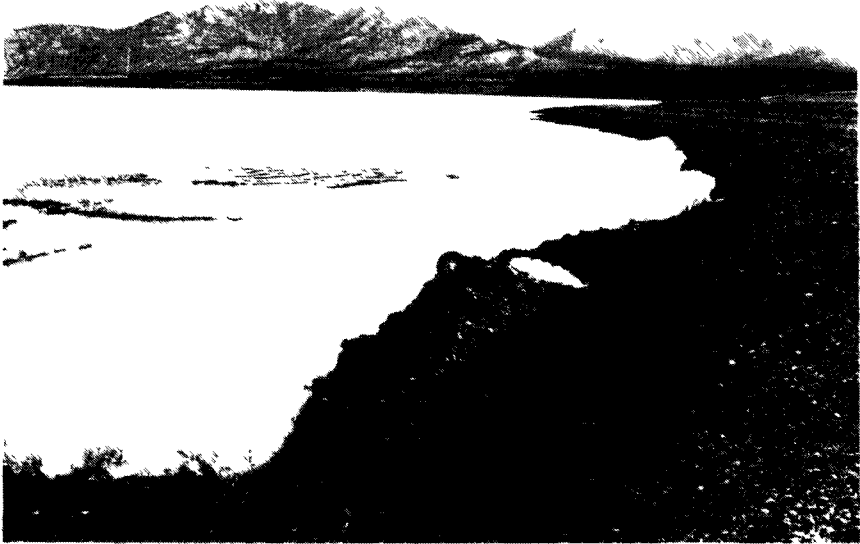


PLATE 22: Ice floe and pushed sediment ridge

TABLE 3

Dimensions of ice floes and corresponding ice-push ridges

		May 29	May 30	June 1	June 1
		I C E	length (down beach)	45.0 m	68.5 m
	width (offshore)	undetermined	22.0 m	1.52 to 2.97 m	3.20 m
	thickness	0.10 to 8.18 m	0.30 to 0.46 m	0.15 to 0.25 m	0.30 m
P U S H R I D G E	length (down beach)	45.0 m	3.6 m	5.64 m	3.05 m
	width	undetermined	0.49 m	2.54 to 4.57 m	0.41 to 0.61 m
	height	0.08 to 0.18 m	0.30 m	0.15 to 0.43 m	0.46 m
C O M M E N T S	Silver City AINA beach site AINA beach site AINA beach site Part of major ice flow that was push- Push-ridge located ed ashore by strong just offshore Ice-push ridge I Ice-push ridge II southwest winds.				

TABLE 4

Sediment sorting characteristics of ice-push ridges I and II

Profile lines		Rows					
		A	B	C	D	E	F
1	\bar{X}	-1.08	-1.27	-1.00	-1.70	-1.37	-2.07
	σ	1.85	-	-	1.60	-	1.42
	v	poor	-	-	poor	-	poor
2	\bar{X}	-1.10	-	-0.90	-0.50	-1.57	-3.40
	σ	1.81	-	(1.78)	1.57	(2.7)	-
	v	poor	-	(poor)	poor	(very poor)	-

Ice-push ridge I

Profile lines		Rows			
		A	B	C	D
1	\bar{X}	-0.73	1.07	-	-0.93
	σ	1.73	1.60	-	-
	v	poor	poor	-	-
2	\bar{X}	-1.58	-0.95	-0.73	-0.93
	σ	1.13	1.55	(2.0)	-
	v	poor	poor	(very poor)	-

Ice-push ridge II

(\bar{X} , mean in phi size units; σ , standard deviation; v, verbal statement on sorting)

the undisturbed sediment and a cross-section of the ridge (Plate 23) showed the uniform distribution of the poorly sorted sediment throughout the ridge. The cross section further revealed the leading edge of the ice floe, clearly demonstrating the plowing action of the floe. It is, however, very hard to predict the amount of sediment pushed by this method because not only is it necessary to know the type and structure of the ice to determine its crushing strength, but the momentum of the ice as it hits the shore must be calculated to determine the relative amount of potential energy the floe has for work on the sediment. This factor, at the present time, cannot be assessed because of the lack of technology for implementing empirical tests.

As the ice disappears, a few scars remain on the beach as evidence of its work. However, with the dramatic rise in water level through the summer months, all visible traces of the effect of ice on beach sediments disappear. Therefore, the importance of ice on the coastal sediments of Kluane Lake is not in its overall yearly effect, but rather in its dynamic effect through the seasonal cycle of formation, total cover, and breakup.

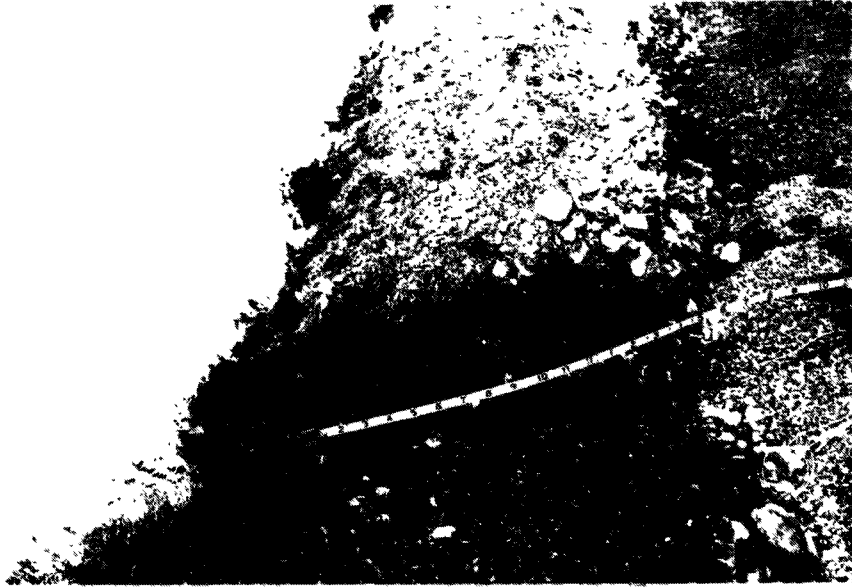


PLATE 23: Cross section of ice push ridge

3. NEARSHORE WATER DYNAMICS

It has long been recognized that wave energy is the most important factor in beach sediment movement in all types of climates, ranging from the Arctic, where beaches may be exposed to wave attack for only two months of the year (Hume and Schalk, 1967), to the Tropics. The predominant wave which affects the coasts is generated from the transfer of energy of wind to the water. The theoretical mechanics of this transfer of energy have been analyzed by assuming that air flows over water in a quasi-laminar fashion (King, 1972). In addition, Phillips (1957) tested the flow of turbulent air over the water and found that it caused a pressure differential on the surface thereby affecting the creation of waves. Waves that originate from wind energy, the bulk of which are classified as gravity waves, are categorized as either seas or swells. Seas are waves which are in the local generating area, and usually are steep, have short periods, and have irregular forms. Swells, however, are waves that have moved out of the generating area, are not subject to any new significant wind action, and generally have a more regular form (Shore Protection Manual, 1973).

The characteristics of length, period, and height of the waves are important in determining the amount of energy they hold (Figure 6). As defined in figure 6, length (L) is the distance between two successive crests, velocity (c) is the rate of movement of the wave form, and period (T) is the time taken for the wave form to move the distance of one wave length. The relationship of these characteristics is,

$$L = cT \tag{3.1}$$

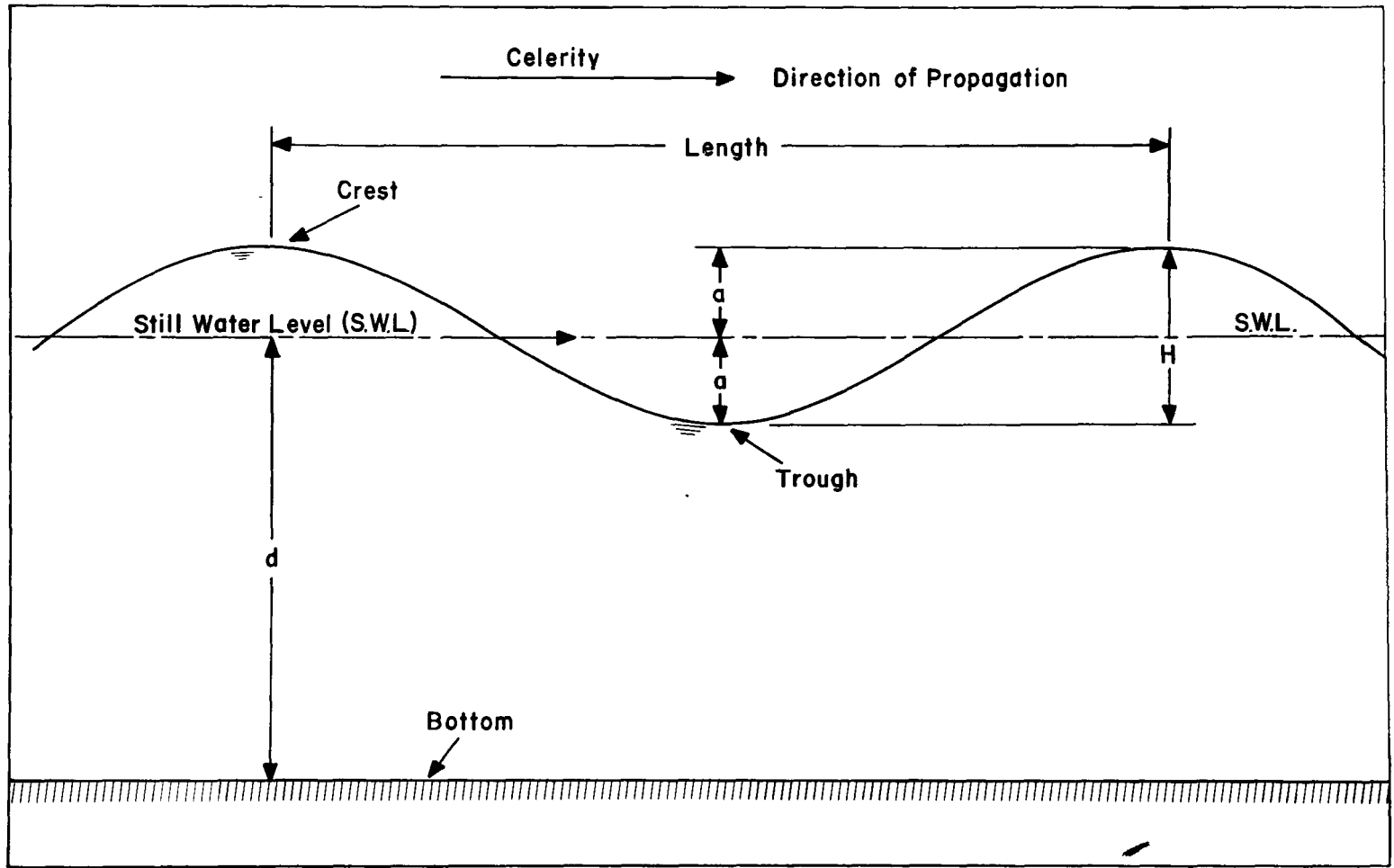


FIGURE 6. DEFINITION OF TERMS (after Shore Protection Manual, 1973)

with the relationship between deep water length (L_o) and period being in meters

$$L_o = 1.56 T^2 \quad (3.2)$$

according to the Airy theory which assumes a sinusoidal wave form. (Shore Protection Manual, 1973). Wave height (H) is measured vertically from the trough to the crest and it is the major determinant of the amount of energy held by the wave. As the wave form moves in deep water, the particles of water which compose the wave move in circular orbits (Figure 7a) and their velocity at the surface depends upon the period and height of the wave. Thus, the diameter of one orbit is equal to the height of the wave over one period. According to the Stokes theory, these orbits are open ended and each water particle advances slightly in the direction of the wave. This is known as the mass movement of the wave and is considered to be very small in comparison with the overall wave and orbital velocities (King, 1972). These Stokes higher order theories give a more accurate account of mass movement, velocity, and pressure fields due to waves if accurate values of period and amplitude are known. However,

"the uncertainty about the accurate wave height and period leads to greater uncertainty about the ultimate answer than does neglecting the effect of nonlinear processes. Thus it is unlikely the extra work involved in using nonlinear theories is justified." (Shore Protection Manual, 1973, p. 2-33)

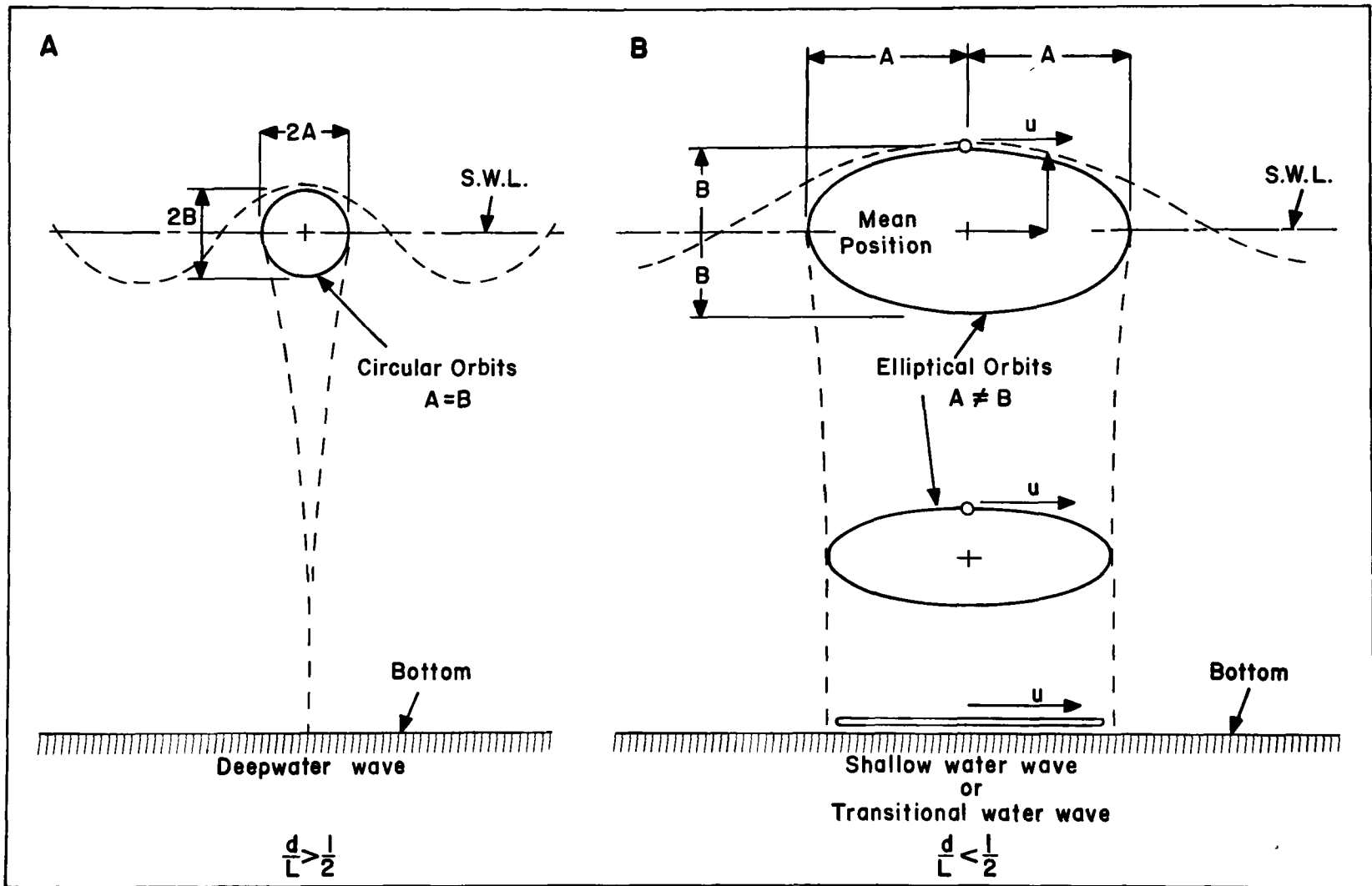


FIGURE 7. WATER PARTICLE DISPLACEMENTS FROM MEAN POSITION FOR SHALLOW-WATER AND DEEPWATER WAVES. (after Shore Protection Manual, 1973.)

As the waves approach shallow water, defined by the depth of water (d) being less than one half of the wave length, their characteristics change considerably. Although the period remains constant, both the length and velocity decrease in proportion. The velocity eventually becomes more dependent upon the depth up to the point where,

$$c^2 = gd \quad (3.3)$$

where,

g is acceleration due to gravity

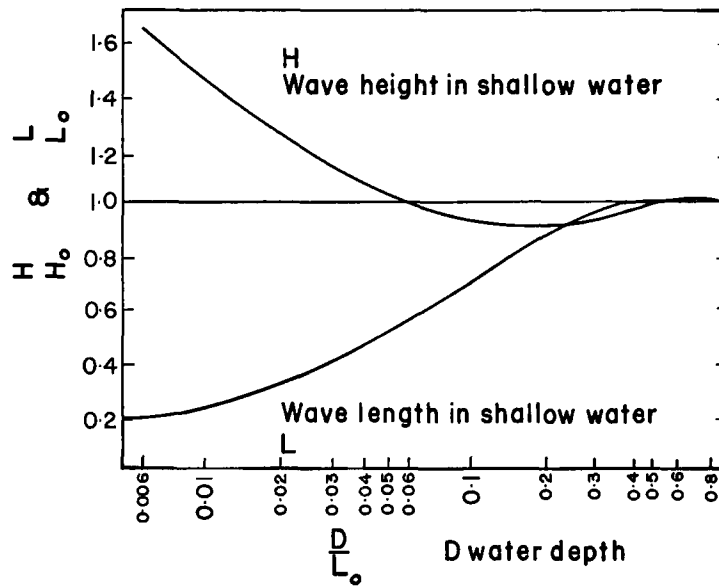
Other changes of wave characteristics which occur in shallow water include an increasing height, the trough between the crests becoming long and flat, and an increasing wave steepness, or the ratio between height and length, H/L , becoming large as depicted in figure 8. The dynamic properties of the wave change as well. The orbital path of the wave particles becomes more elliptical (Figure 7b), and because of the reduction in depth the waves become prone to refraction, or bending. This property of refraction results in either a concentration of energy on one area of the shoreline or a spreading out of the wave energy over a wide area when the wave travels over irregular bottom contours or approaches headland features (Figure 9). This is a major factor in determining whether a coastline is erosional or accretionary.

The total energy of a breaking wave (E_T) is equal to its kinetic energy (E_K) or the energy of its dynamic movement, plus its potential energy (E_P). This relationship is,

$$E_T = E_K + E_P \quad (3.4)$$

or,

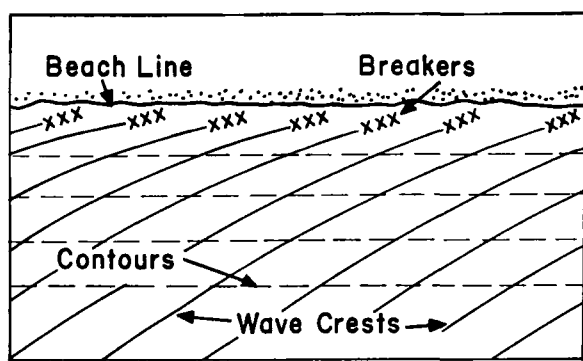
$$E_T = \frac{\rho g H_b^2 L_b}{16} + \frac{\rho g H_b^2 L_b}{16} = \frac{\rho g H_b^2 L_b}{8} \quad (3.5)$$



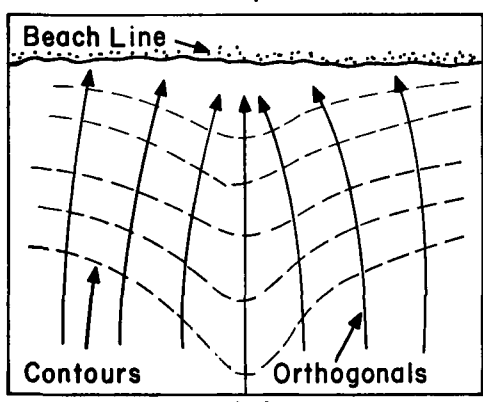
° Refers to deep water value

FIGURE 8. THE CHANGE OF WAVE LENGTH AND WAVE HEIGHT IN RELATION TO THE RATIO OF DEPTH TO WAVE LENGTH.

(after King, 1972.)

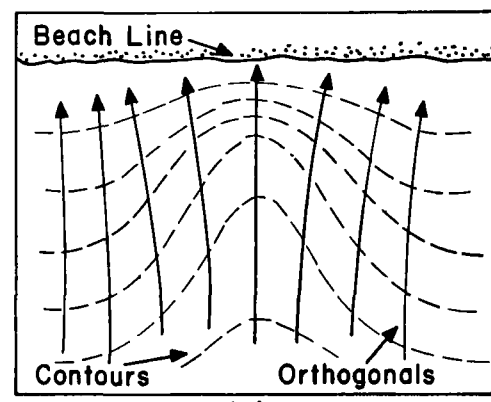


(A) Refraction along a straight beach with parallel bottom contours.



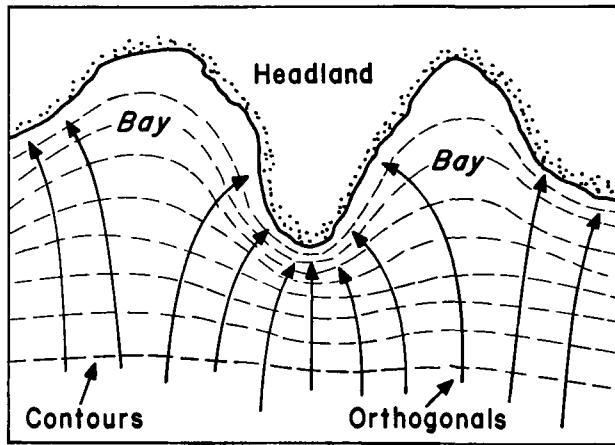
(B)

Refraction by a submarine ridge.



(C)

Refraction by a submarine canyon.



(D) Refraction along an irregular shoreline.

FIGURE 9. WAVE REFRACTION PATTERNS
(after Shore Protection Manual, 1973)

where, ρ is the density of water

H_b is the height of the breaking wave

L_b is the length of the breaking wave

The average energy density (\bar{E}) per unit surface area of the wave is therefore,

$$\bar{E} = \frac{\rho g H_b^2}{8} \quad (3.6)$$

The wave energy flux (P), defined as the rate which energy is transmitted in the direction of wave propagation across a vertical plane perpendicular to the direction of the wave advance extending down the entire depth (Shore Protection Manual, 1973), is equal to the energy density (E) times the group velocity of the wave train (c_g) or the rate at which energy propagates. The change in direction caused by refraction can be found through Snell's Law,

$$\sin \theta_2 = \sin \theta_1 \frac{c_2}{c_1} \quad (3.7)$$

where,

θ , is the angle the wave makes with a bottom contour over which it is passing at a velocity c_1 , and θ_2 is the changed angle as the wave passes the next contour at a velocity c_2 .

The relationship may help determine the change and concentration of wave energy flux along a coastline. Because the AINA beach site had a straight beach form and nearly parallel bottom contour lines, it can be assumed that there was little variation of wave energy along the beach due to refraction.

Within literature, four types of breaking waves have been identified based upon the manner in which they break (Patrick and Wiegand, 1955; Wiegand, 1964; Galvin, 1968; and Shore Protection Manual, 1973): first, the

spilling breaker which has been characterized by having a white crest which "spills" onto the front face of the wave causing a wide swash zone; second, the plunging breaker which has a curl crest and plunges forward providing for a much smaller swash zone width; third and fourth, surging and collapsing breakers which maybe considered transitional waves. The former builds up as a plunging wave but its base surges before the crest can plunge forward creating a large swash zone. The latter also builds up as a plunging wave but suddenly collapses creating a very small swash zone. All four types of waves were observed at Kluane Lake. It was also observed that the waves that created the wide sweeping swash zone, such as the spilling and surging waves, were most effective in creating longshore movement of sediment, while the plunging wave mixed the sediment by burying the surficial sand and the collapsing wave made only a minor disturbance.

As the wave crests approach the shore at an angle, the energy flux takes on a longshore component thus driving a longshore current of water. This current moves parallel with the shoreline and is generally confined between the zone of breaking waves and the edge of the swash zone. Its velocity is dependent upon the angle of the wave crest to the shore and the height of the wave crest at breaking (Shore Protection Manual, 1973). This current is not, however, similar to a river of water running alongshore but it is broken up into cells (Shepard and Inman, 1950; Inman and Bagnold, 1963; Komar, 1970; Tanner, 1973). These cells have been reported to behave differently in high energy regimes from those in lower energy regimes. Under high energy, the longshore current begins very slowly and accelerates to a critical velocity when it is forced seaward by a rip current (Figure 10). The definition of a

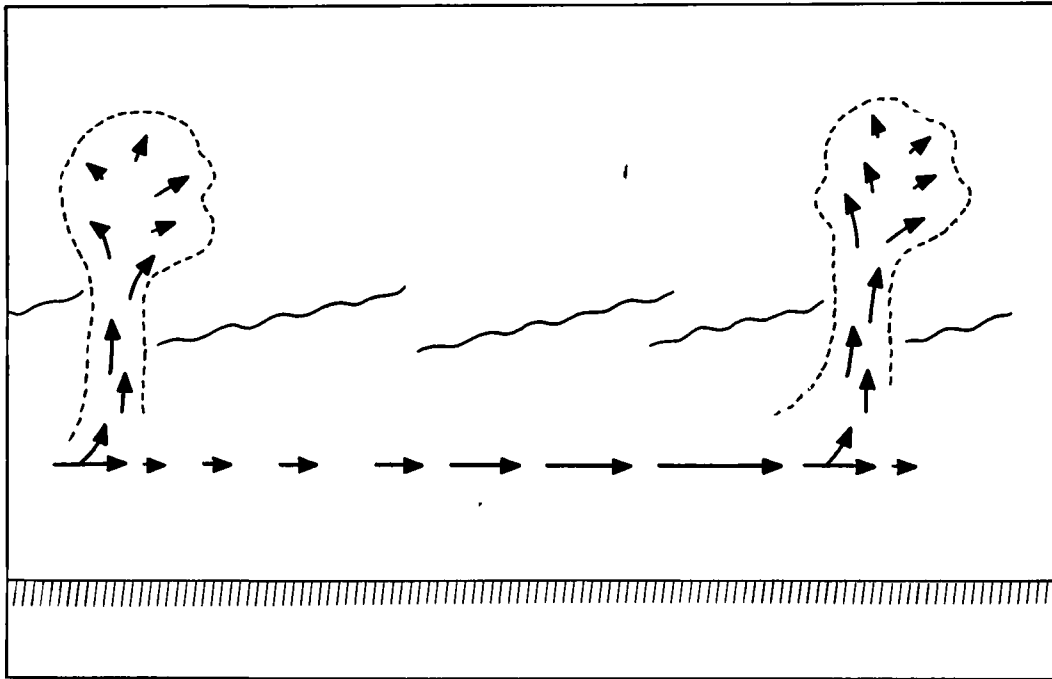


FIGURE 10. SCHEMATIC DIAGRAM OF RIP CURRENTS
(after Komar, 1969)

circulation cell in low energy, according to Tanner (1973), is,

"the area covered by one erosional volume plus one depositional volume, plus a transport section in between."
(p. 24)

He adds that one cell may contain a number of smaller cells or subcells, but the total compartment cell is an isolated entity. Tanner also points out that the major causative factors of the origin of these cells are shore features and submarine bars. The literature does not agree on the size of the cells. Inman and Bagnold (1963) report that the distance between rip currents during a period of low waves ranged from 30 m to 1000 m whereas Tanner (1973) found cells off the Florida coast, a low energy environment, ranging 1 km to 10 km. In any case, because the size of the study site at the AINA beach was not more than 10 m, the only importance the cells could have is an explanation for the variance in the field data on longshore current velocities.

There have been many attempts to formulate a predictive equation for longshore current velocity. Galvin (1967) made a complete review of the major theories, and classified them into three types of approaches: conservation of momentum and energy, conservation of mass, and the empirical correlation of data. The most prominent of the first group was the pioneer work done by Putnam, Munk, and Traylor (1949). Based on tests in a laboratory wave tank and field data from other sources, they calculated two prediction equations, one by an energy approach and one by a momentum approach. The energy equation was developed from the solitary wave theory in which the average longshore current velocity (V) depended upon the breaker height (H_b), the wave period (T), the angle of incidence of the wave crest to the shore (α), the beach slope (m), and a coefficient of friction (C_f) by the following relationship (Figure 11):

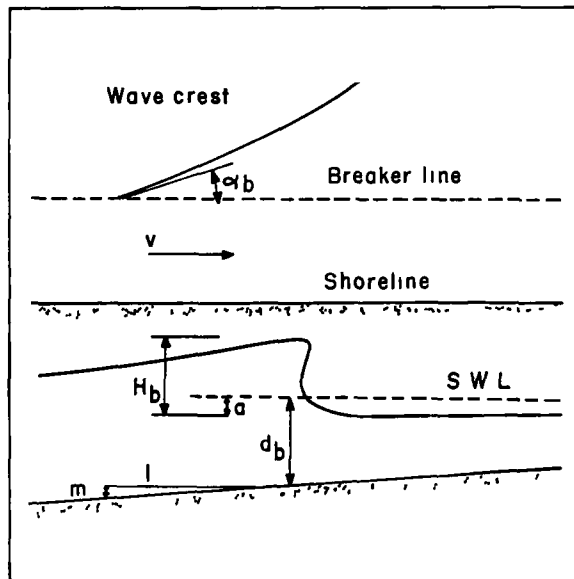


FIGURE II. DEFINITION OF VARIABLES
OF A BREAKING WAVE
(after Galvin, 1967.)

$$v = C_f \left[(mH_b^2/T) \right] \sin 2\alpha \quad (3.8)$$

where,

$$C_f^3 = 0.871 \text{ g s/k} \quad (3.9)$$

where, s is the small fraction of energy responsible for setting up longshore currents
 K is the hydraulic roughness of the beach

Putnam et al, (1949) point out that this equation applies only to the situation in which the waves are breaking over a long enough period to set up a steady state environment in a region which is far from any obstruction so that full current velocity can be reached. The momentum equation was developed with consideration of the momentum of the mass of water alongshore. They reasoned that with every breaking wave, a certain water mass is thrown into motion in the direction of wave propagation, and the longshore component of this motion provides the driving force for the longshore current. With this underlying principle they developed the following relationships:

$$v = (a/2) \left[(1 + 4\epsilon \sin \alpha/a)^{\frac{1}{2}} - 1 \right] \quad (3.10)$$

where,

$$a = (2.61 m H_b \cos \alpha)/C_f T \quad (3.11)$$

This equation had the same limitations as the energy equation. Longuet-Higgins (1970) regarded the momentum equation as a truer representation of the driving force behind the longshore velocity of water because unlike energy, momentum is conserved. Galvin (1967), however, found both of these equations impractical because first, the flux assigned to the longshore current has been found to be a small fraction, less than 0.1, and often less than 0.01, of the flux of the incident waves, second, the energy flux on the current is not a constant fraction of the incident flux, and third, the computed flux in the unsteady uniform current depends upon coefficients analogous to

empirical coefficients measured in steady open channel flow.

Longshore current velocity prediction equations by Inman and Bagnold (1963) were derived by utilizing the principle of conservation of mass. Inman and Bagnold pointed out many discrepancies in the Putnam et al equations by citing common field conditions which were not accounted for, such as the drag coefficient varying unaccountably by a factor exceeding 10^4 , the presence of rip currents, and the longshore currents which do not achieve steady flow but are constantly fluctuating in response to the periodicity of the grouping of higher and lower waves. They hypothesized that since longshore currents are pulsating, the remaining longshore component of momentum flux is extended by accelerating the water mass from near rest to a maximum velocity when it turns seaward in the form of a rip current. On the basis of this hypothesis, the following relationship was developed:

$$\bar{V} = 4[(\gamma/3)(l/T)]^{1/2} \tan \eta \sin \alpha \cos \alpha \quad (3.12)$$

where,

- \bar{V} is the average longshore current velocity
- γ is the ratio of the breaking height of the wave (H_b) to the water depth at breaking (d_b)
- η is the angle of the slope of the beachface
- l is the distance between rip currents

Galvin (1967) commented that this approach was more practical than the momentum energy flux model because longshore current was the most dominant mass flow in the surf zone. This is particularly true for low-energy flows where observation indicates that the current is merely the averaged longshore component of the surge induced water particle motion. He concluded, however, that the approximations in this theory, the distance between rip currents for example, were extreme.

Prediction equations developed from empirical correlations of data have been derived by Inman and Quinn (1951), Brebner and Kamphuis (1963) and Harrison and Krumbein (1964) by performing linear multiple regression analysis in deep water field data. They found that six out of eleven variables cause the greatest reduction of variability of predicted longshore current velocities. Galvin (1967) thought that this method showed the most promise but there was very little reliable data available to derive an accurate prediction equation. This was the critical area for developing more accurate equations for predicting the velocities of longshore currents.

From this background, Longuet-Higgins (1970a) developed an equation for prediction of longshore current velocity based upon the principle of radiation stress and the small amplitude Airy wave theory. By incorporating the theory of radiation stress (Longuet-Higgins and Stewart, 1964), he found that the net bottom friction stress in the longshore direction (B_Y) is equal to the stress per unit length exerted by waves on the water in the surf zone (τ_Y) or:

$$\bar{B}_Y = \tau_Y \quad (3.13)$$

$$\text{or,} \quad 2/\pi C_f (\rho U_m \bar{V}) = \rho U_m^2 (m \sin \alpha) \quad (3.14)$$

$$\text{or,} \quad \bar{V} = \frac{5\pi}{8 C_f} U_m (m \sin \alpha) \quad (3.15)$$

where,

U_m is the maximum horizontal velocity of a water particle within the wave

This relationship implies that for constant values of C_f and m , the longshore current velocity is proportional to the longshore component of the orbital velocity. By the linear Airy theory and the definition of γ , which is the

ratio between the wave amplitude at breaking (a_b), and the water depth at breaking (d_b), U_m can be defined by the relationship:

$$U_m = \gamma (gd_b)^{\frac{1}{2}} \quad (3.16)$$

and equation (3.17) can be changed to:

$$V = \frac{5\pi}{8} \left(\frac{\gamma}{C_f} \right) (gd_b)^{\frac{1}{2}} (m \sin \alpha) \quad (3.17)$$

This equation describes the longshore current velocity for spilling breakers as being at a maximum just as the wave breaks and in constant decline through the swash zone. A horizontal mixing factor (β), which is a certain function of the width of the breaking wave or a theoretical horizontal mixing length, and the width of the swash zone, rounds out this curve and places the maximum velocity just landward of the breaking wave (Longuet-Higgins, 1970a). Thus, by adding this factor and substituting $(H_b/2\gamma)^{\frac{1}{2}}$ for $(d_b)^{\frac{1}{2}}$, since the breaking height is a more common observed field parameter than the depth of water at breaking, the final equation,

$$V = \frac{(5\pi)}{8} \frac{(\gamma\beta)}{(2)^{\frac{1}{2}}(C_f)} (gH_b)^{\frac{1}{2}} (m \sin \alpha) \quad (3.18)$$

is arrived at. Further clarification of the coefficient of friction (C_f) was needed however. In his derivation, Longuet-Higgins (1970a) suggested that the values for C_f could be taken from a graph developed by Prandtl (1952). This graph correlated the Reynolds number and the ratio of the length of the experimental plate (l_p) to the scale of roughness of the bed (k) to

the coefficient of friction based on Nikuradse's experiments of flow of water through roughened pipes. From this graph, Longuet-Higgins argued that the values for the coefficient of friction of low energy waves can be taken at .01 or the limit of Prandtl's graph. Schlichting (1955), however, expanded this graph and extrapolated the following equation for C_f :

$$C_f = (1.89 + 1.62 \log l_p / k)^{-2.5} \quad (3.19)$$

where,

$$l_p = U_m / \sigma \quad (3.20)$$

where, σ is ^{u.} the wave frequency in radians
 $K \cdot 10^{-3}$ m average grain size

This equation gave values significantly greater than 0.01 for low energy conditions. Therefore, it is proposed that under low energy environments, the role of friction becomes much larger in determining the rate of longshore currents.

Field measurement techniques of wave characteristics, specifically breaker heights, angle of incidence of the waves to the shore, and wave period, have developed slowly through the years. King (1966, 1972) and Komar (1969) have described both simple and complex methods of collecting values for these variables. Because of both equipment and transportation costs, only the simplest techniques were used from King (1966) to fit specific field conditions at Kluane Lake. The following methods were not unlike those developed by the Coastal Engineering Research Center in their Littoral Environment Observation (LEO) method (Balsillie, 1975). Wave height at breaking was measured by a pole anchored 3 m offshore and calibrated in 10 cm segments. As the season progressed and the lake water level rose, the pole was moved inshore to make certain that the wave heights were being measured

as close to the breakpoint as possible. The angle of incidence between the wave crest and the shore was measured by a Brunton compass. Readings were recorded by calculating the difference in the compass orientation between the wave crest and the shore. Finally, the period was recorded by counting the number of breaking waves in one minute.

The methods of measuring longshore current velocity have not advanced a great deal since Putnam, Munk, and Traylor (1949) timed the rate of movement of fluorescent dye and a float alongshore within the surf zone. Subsequent studies (Inman and Quinn, 1951; Galvin and Savage, 1966; Inman and Bagnold, 1963) used either these techniques or such traceable objects as weighted balloons and seaweed. Even as late as 1975, there were no new technological advances in recording equipment (Galvin, personal communication). The longshore current velocity at Kluane Lake was measured by calculating the rate of a weighted cork over a 5 or 10 m distance, the length of the distance being dependent upon the amount of wave energy present at the time of measurement. The procedure was to place the weighted cork just beyond the zone of breaking waves and to time the rate of movement through the measured length and the surf zone.

Readings of both wave characteristics and longshore current velocities were spot measurements and were not designed to reflect average conditions over a period of time. For example, on days when calm conditions prevailed on the lake surface no readings were obtained, whereas on days of significant wave activity, e.g. wave heights over 15 cm, usually two sets of data were taken. The data, therefore, do not constitute a time series. Values of wave height, angle of wave approach, wave period, depth of breaking and observed longshore current velocity are displayed in table 5.

TABLE 5

Wave characteristics, AINA beach site 1975

DATE		H_b (m)	α °	T (sec)	d_b (m)	Observed L.C.V. (m / sec.)
		± 0.03	± 4	± 0.01	± 0.03	± 0.03
July	5	0.24	18	3.0	0.38	0.22
	5	0.30	22	3.2	0.38	0.29
	8	0.09	10	2.1	0.10	0.10
	9	0.11	15	2.4	0.10	0.13
	11	0.05	11	1.2	0.05	0.04
	11	0.20	17	2.3	0.18	0.17
	12	0.07	17	1.6	0.18	0.12
	13	0.10	12	1.9	0.18	0.20
	14	0.03	22	1.5	0.08	0.09
	15	0.08	16	1.8	0.18	0.15
	16	0.04	10	1.7	0.08	0.06
	18	0.32	13	2.4	0.68	0.30
	19	0.09	10	1.9	0.48	0.11
	23	0.10	17	1.7	0.25	0.11
	24	0.17	10	2.1	0.30	0.15
	24	0.24	16	2.2	0.50	0.23
	25	0.11	15	1.9	0.35	0.13
	28	0.18	18	2.1	0.35	0.16
	28	0.60	25	3.0	0.95	1.25
	30	0.08	7	1.7	0.20	0.08
30	0.20	15	1.1	0.35	0.22	
31	0.18	13	2.0	0.35	0.22	
31	0.28	15	2.1	0.40	0.24	
August	1	0.14	13	1.9	0.28	0.17
	2	0.11	15	1.6	0.20	0.12
	2	0.20	20	2.7	0.35	0.37
	3	0.52	15	3.3	0.98	0.56
	3	0.40	16	3.0	0.98	0.21
	4	0.11	14	2.4	0.30	0.13
	5	0.18	17	2.4	0.42	0.15
	6	0.18	15	2.7	0.42	0.18
	8	0.18	11	2.1	0.44	0.17
	10	0.11	11	1.9	0.28	0.08

(H_b , breaker height; α , angle of wave approach; T, wave period; d_b , depth at breaking)

Through the use of these wave characteristics together with the coefficients of friction and horizontal mixing, the Longuet-Higgins equation (3.18) was employed to predict a longshore current velocity (Table 6). The values of the coefficient of friction were calculated by the Schlichting equation (3.19) through consideration of wave characteristics, depth of water in the breaker zone, and observed surficial sediment size within the foreshore zone (Table 6). The value of the horizontal mixing coefficient was taken as 0.167 (Longuet-Higgins, 1970a, p. 6785) because of the very small swash zone that was apparent at the AINA beach site.

The relation between observed and predicted longshore current velocities (Table 6) was tested by simple linear regression techniques. A correlation coefficient (r) of 0.926 was obtained. Regression analysis resulted in a slope of +0.916 between the data (Figure 12). The regression was significant at the 95% confidence level (Students $t' = 36.17$; d.f. = 31). In addition through the Durbin-Watson and graphic analysis, it was shown that there was no autocorrelation or heteroscedasticity with the error terms of the regression. When the constant value of 0.01 was used for the coefficient of friction, as suggested by Longuet-Higgins (1970a), the slope of the regression line between observed and computed longshore current velocities was +0.615 with a correlation coefficient of 0.992.

This analysis indicates, therefore, that the Longuet-Higgins equation derived from high-energy conditions is a good predictive equation for low-energy conditions when a variable coefficient of friction is used. It was also probable, from these results, that the accuracy of prediction in high energy environments could be improved with a variable coefficient of friction.

TABLE 6

Summary of data for calculation of predicted
longshore current velocities AINA beach site

DATE	m ^{1.} $\tan \eta$	H_b/d_b ^{2.}	C_f ^{3.} Schlichting	Predicted ^{4.} L.C.V. (m/sec.)	Observed L.C.V. (m/sec.)	
July	5	0.037	0.63	0.0129	0.24	0.22
	5	0.037	0.78	0.0118	0.43	0.29
	8	0.037	0.90	0.0166	0.08	0.10
	9	0.037	1.10	0.0152	0.16	0.23
	11	0.037	1.00	0.0223	0.03	0.04
	11	0.075	1.12	0.0231	0.16	0.17
	12	0.075	0.39	0.0202	0.15	0.22
	13	0.075	0.60	0.0181	0.15	0.20
	14	0.075	0.33	0.0285	0.07	0.09
	15	0.075	0.48	0.0198	0.14	0.15
	16	0.075	0.53	0.0251	0.05	0.06
	18	0.075	0.43	0.0178	0.25	0.30
	19	0.075	0.20	0.0298	0.05	0.11
	23	0.075	0.38	0.0260	0.13	0.11
	24	0.075	0.58	0.0201	0.17	0.15
	24	0.075	0.47	0.0195	0.30	0.23
	25	0.075	0.31	0.0258	0.11	0.13
	28	0.075	0.50	0.0200	0.30	0.16
	28	0.075	0.63	0.0133	0.24	1.25
	30	0.075	0.40	0.0215	0.07	0.08
	30	0.075	0.57	0.0154	0.35	0.22
	31	0.075	0.50	0.0186	0.24	0.22
	31	0.075	0.59	0.0161	0.38	0.24
August	1	0.075	0.49	0.0235	0.16	0.17
	2	0.075	0.55	0.0261	0.15	0.12
	2	0.075	0.64	0.0187	0.43	0.37
	3	0.075	0.54	0.0139	0.63	0.56
	3	0.075	0.41	0.0177	0.40	0.21
	4	0.075	0.37	0.0218	0.20	0.13
	5	0.075	0.41	0.0233	0.31	0.15
	6	0.075	0.44	0.0196	0.34	0.18
	8	0.075	0.54	0.0208	0.26	0.17
	10	0.075	0.40	0.0340	0.11	0.08

1. taken from profiles Figure 2
2. H_b and d_b from Table 5
3. see equation 3.19 (p. 61)
4. see equation 3.18 (p. 60)

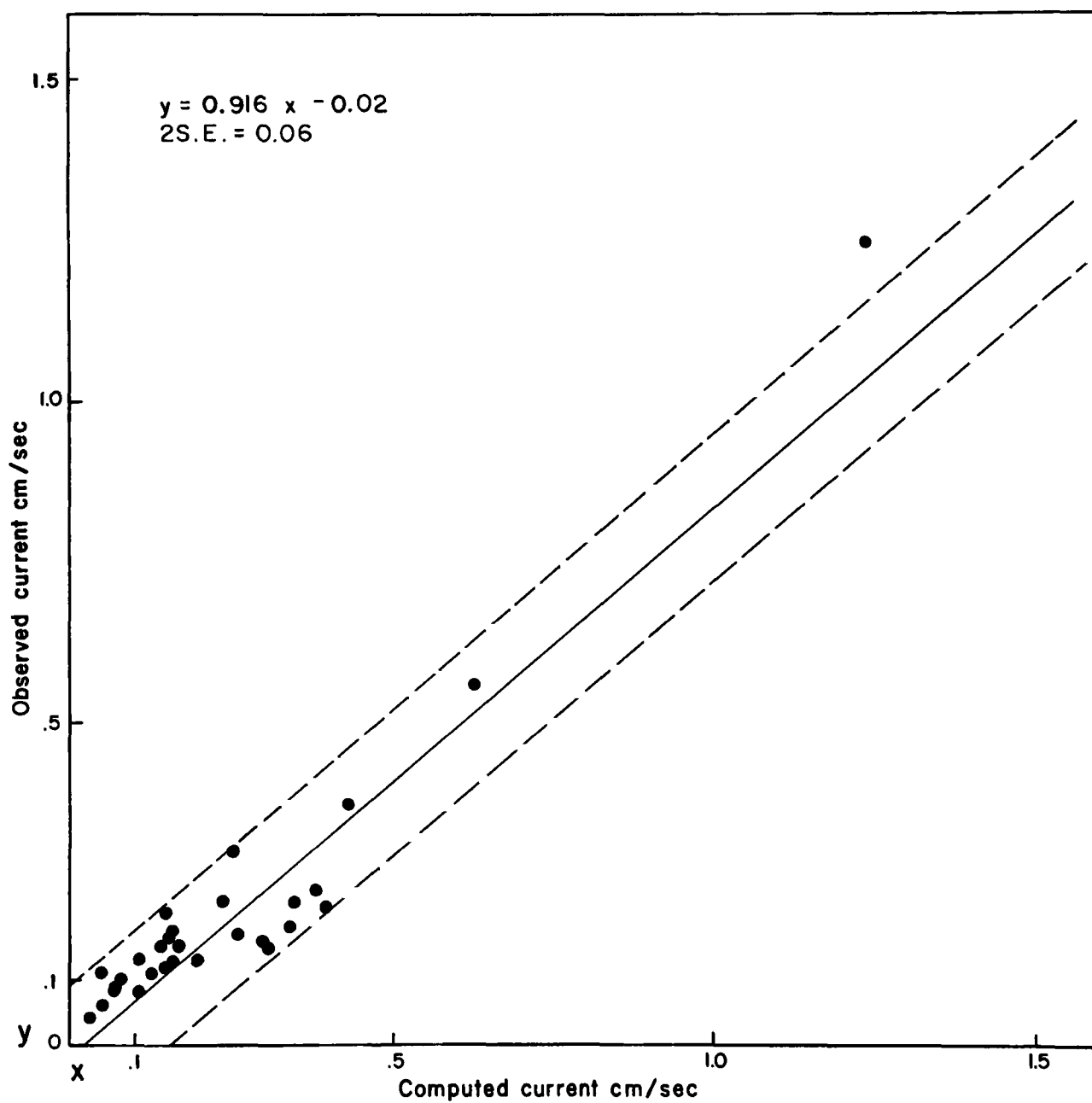


FIGURE 12. RELATIONSHIP BETWEEN OBSERVED AND COMPUTED LONGSHORE CURRENT VELOCITIES

4. LONGSHORE SEDIMENT TRANSPORT BY WAVE ACTION

The nearshore water dynamics of waves and longshore currents generate the transport mechanisms of the beachface. These mechanisms act within an area between the shoreline and just offshore of the breaker area. This area is referred to as the littoral zone and the movement of sediment within this zone is called littoral transport (Figure 13) (Shore Protection Manual, 1973). There are two directions in which the sediment moves in this zone, onshore-offshore where the net direction is perpendicular to the shore, and alongshore where the net direction is parallel to the shoreline. Each of these directions is important in determining the form of the beach and whether it is an erosional or accretionary beach. The research design of this study was aimed primarily at the longshore transport component.

The major portion of longshore transport of sediment occurs between the upper edge of the swash zone and the breaker zone, which is also where the velocity of longshore currents is the greatest. Komar (1971) defined the mechanics of this transport.

"Sediment moves forward obliquely up the beach under the action of the breaking wave and swash. This is followed by a seaward transport of sediment normal to the shoreline under gravity-driven return flow. The resulting longshore movement of sediment is usually described as saw-tooth. The littoral drift results from the longshore component of the movement of sediment forward under the advancing swash." (p. 715)

Figure (14) depicts this definition of the saw-tooth motion of longshore transport. This definition, however, is a generalized picture because both the volume and mechanics of sediment transport alongshore depend upon other variables such as the type of wave action, the strength of longshore current

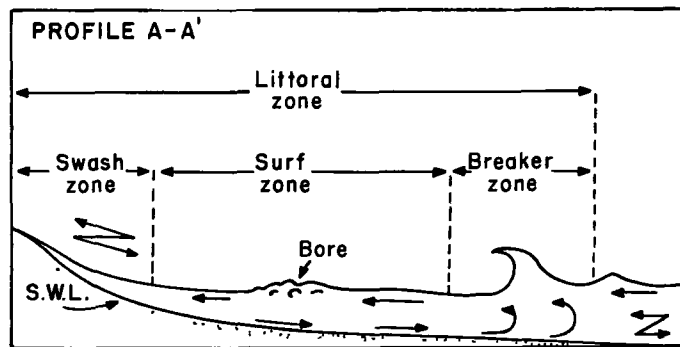


FIGURE 13. TERMINOLOGY OF NEARSHORE
CURRENT SYSTEMS.

(after Ingle, 1966.)

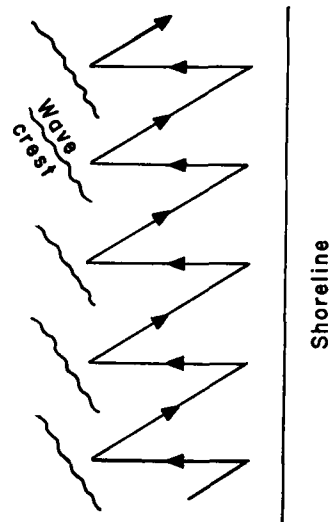


FIGURE 14. SCHEMATIC DIAGRAM OF LONGSHORE
SEDIMENT MOVEMENT.

(after Komar, 1971.)

velocity, the grain size of the sediment and its position on the beach (Ingle, 1966).

A major determining factor in the quantity of sediment transport alongshore is the amount of wave-induced longshore energy (P_{\perp}) that reaches the shore. As modified from Caldwell (1956) the same expression for P_{\perp} was independently arrived at by both Bagnold and Inman (1966) and was described as:

$$P_{\perp} = (E c_g) \sin \alpha \cos \alpha \quad (4.1)$$

where,

E is the energy density

c_g is the local wave group velocity

α is the angle of incidence of the wave to the shoreline

The energy density (E) has been shown to be related to the wave breaker height (H_b), water density (ρ), and acceleration due to gravity (g) by equation (3.6), and the local wave group velocity can be considered equal to the velocity of a single wave in very shallow water and which at break-point becomes a function of depth as expressed by equation (3.3). Longuet-Higgins (1972) argued that the term of longshore component of energy flux is not correct in a physical sense. He explained that it could be better expressed as lateral thrust (P_{LT}) of the wave on the water and sediment inside the surf zone by the relationship:

$$P_{LT} = E (c_g/c) \sin \alpha \cos \alpha \quad (4.2)$$

which he believes is exact and does not depend upon any application of small amplitude theory to waves inside either the breaker or refraction zone. He equated this lateral thrust (P_{LT}) with longshore energy flux (P_1) by:

$$P_1 = E c_g \sin \alpha \cos \alpha = P_{LT} c \quad (4.3)$$

This is the expression for energy that is used in the analysis of longshore sediment movement at Kluane Lake.

The study of longshore sediment movement began with the classic descriptive works of Gilbert (1890) and D.W. Johnson (1919) in which they hypothesized that nearshore water and sediment ran alongshore much like a river. This hypothesis was further developed by Grant (1943) who noted that the longshore current coupled with the agitating motion of the waves governed the rate of sediment movement, and J.W. Johnson (1956) who quantified the sediment advection rates of the coasts of the United States and depicted how this littoral transport was affected by certain coastal engineering projects. It was Caldwell (1956), however, who first developed a prediction equation based on the relationship between the volume of sediment transported (S) and the amount of longshore energy flux (P_1) available:

$$S = 210 [P \sin \alpha \cos \alpha]^{0.8} = 210 P_1^{0.8} \quad (4.4)$$

Savage (1959) modified this equation by **making** the exponent equal to 1 so that it took the form of:

$$S = 125 P_1 \quad (4.5)$$

Inman and Bagnold (1963) stated that these early attempts at prediction equations were not correct because volume can not be equated with energy or power. Therefore, they converted the volume variable to alongshore dynamic transport rate of immersed weight (I) in which:

$$I = (\rho_s - \rho) g p' S = (\text{a constant}) (P_1) \quad (4.6)$$

where,

ρ_s is the **bulk** density of the sediment

ρ is the density of water

p' is the pore space correction factor

The new constant was nondimensional and was defined as an efficiency coefficient where it estimated the proportionality between the total amount of work done to the total amount of energy available. This constant, therefore, would include such variables as the type of breaking wave (λ), the angle of the slope of the beachface (η), the intergranular coefficient of friction (ϕ) that would affect its value of efficiency. By combining these variables with equation (4.6) the new relationship would be:

$$I = \frac{8}{3 \lambda} \frac{\tan \eta}{\tan \phi} K \frac{l}{cT} P_1 \cos \alpha \quad (4.7)$$

where,

l is the spacing between rip currents

K is the coefficient of proportionality

Ingle (1966) used a different approach and developed a relationship which could determine the relative importance of grain size to proportionality between energy and the rate of longshore sediment movement.

The average rate of sediment transport (\bar{Q}_i) in cubic feet per day was calculated by:

$$\bar{Q}_i = S_w \bar{U}_g \cdot 1440 \quad (4.8)$$

where,

S_w is the unit volume of sand transport in cubic feet/foot of beach ($S_w = DX_b X_L$)
 \bar{U}_g is the average grain velocity per hour alongshore

The value for the depth of the mobile bed layer (D) was then needed to obtain a value for S_w . This was determined by:

$$D = \frac{12 \bar{Q}_i}{\bar{U}_{ga} \cdot A} \quad (4.9)$$

where,

\bar{Q}_i is the known average annual rate of littoral drift for the area
 A is the average annual rate of transport of sand
 \bar{U}_{ga} is the average annual tracer grain velocity (ft/hr)

The other variables needed for S_w were a unit beach length (X_1) and the width of the foreshore-inshore zone (X_b). From a number of tests, Ingle found that the difference of grain size of the sediment of the beachface is **consequential** to the rate of sediment transport in these areas. First, the average grain diameter of the beach determines the thickness of the mobile bed layer which is an integral part of the rate of sediment movement. Second, the mean grain diameter determines the roughness of the bed surface, affecting the flow of water above it, which in turn affects the lift and drag of the sediment particles. Third, following the reasoning put forward by Inman (1949), an increasing amount of incident wave energy or power is

needed to sustain a given rate of sediment transport of increasing grain diameters of more than 1.00 mm, because of the increased bed roughness caused by the coarser grains.

Komar (1969) further developed and substantiated equation (4.6) by defining certain parameters for the rate of volume of sediment transported (S) and collecting field data providing values for the variables involved. The rate of volume of sediment transported was defined and described by the equation:

$$S = D X_b \bar{U}_g \quad (4.10)$$

To attain values of the coefficient of proportionality (K) between I and P Komar used two models. The first model was identical to the one proposed by Inman and Bagnold (1963) and through the relationship

$$I = K P_1 \quad (4.11)$$

it was primarily concerned with the wave power along the coast. The second model,

$$I = K' P \frac{V}{u_m} \quad (4.12)$$

where,

- P is the energy flux on the shoreline disregarding direction
- V is the longshore current velocity
- K' is the coefficient of proportionality
- u_m is the maximum horizontal orbital

related the longshore current velocity with the immersed weight sediment transport rate. Through the use of field values, Komar graphed I versus

P_1 and found K to be equal to 0.77 and K' equal to .28. He therefore inferred from this difference of values that the immersed weight transport rate was directly proportional to PV/U_{max} based on the concept that wave action causes stress to initiate sediment disturbance while the longshore current causes the transport of the agitated sediment. He further reasoned that the current and wave models are not independent but rather equivalent because the longshore current velocity (V) is a function of both wave breaking height and the angle of approach to the shore. Therefore, by sorting equations (4.11) and (4.12) simultaneously to eliminate I , the relationship

$$V = \frac{K}{K'} u_m \sin \alpha \cos \alpha \quad (4.13)$$

was obtained where both K and K' are independent of the coefficient of friction and beach slope. Komar therefore concluded from this analysis that the water motion which is of importance to the longshore transport of sand is the wave bore and swash which approach the shoreline at an angle and return in a direction normal to it. This would result in a net drift of sediment alongshore.

Longuet-Higgins postulated different interpretations for K and K' . By equating the tangential stress on the beach with a hypothetical coefficient of friction (C_f') of the moving sand over the beachface and the immersed weight of mobile sand (I_w) he redefined the lateral thrust of water alongshore (P_{LT}) as:

$$P_{LT} = C_f' I w \sin \delta \quad (4.14)$$

where,

δ is a small angle to the normal of the shoreline

Then, by assuming that the pattern of longshore sediment transport resembles a distorted sine-wave, he proposed that δ is of the order \bar{U}_g/U_s where U_s is the maximum onshore-offshore velocity of sediment. Further, assuming that U_s is nearly equal to $\frac{1}{2} (gd_b)^{\frac{1}{2}}$ and the mean value of $d_b^{-\frac{1}{2}}$ for a uniform beach slope is $\frac{1}{2} d_b^{-\frac{1}{2}}$, he noted that

$$P_{LT} \sim 4C_f' I w \bar{U}_g / (gd_b)^{\frac{1}{2}} \quad (4.15)$$

or,

$$P_{LT} (gd_b)^{\frac{1}{2}} \sim 4C_f' I \quad (4.16)$$

where,

$$I = I w \bar{U}_g \quad (4.17)$$

From equation (3.3), in which $c = (gd_b)^{\frac{1}{2}}$, by incorporating equation (4.11) and (4.15), and assuming Komar's (1969) value for K is correct, he further noted that

$$4C_f' \sim K^{-1} = 1.3 \quad (4.18)$$

From this reasoning, Longuet-Higgins established a relationship between the coefficient of friction of the sediment and the coefficient of proportionality (K). In analyzing K' , Longuet-Higgins (1972) disputed Komar and Inman's (1970) basic assumptions that a fixed proportion of wave energy flux was used to

transport sand up and down the beach and that the sand was being carried along with a velocity directly proportional to the longshore current velocity. He argued that because most of the energy flux goes into the action of the wave breaking, only very little is left for the transport of sand and therefore there seemed little reason to accept the first assumption. Because the sand is assumed to be transported alongshore with a velocity directly proportional to the longshore current velocity, as stated in the second assumption by Komar and Inman, Longuet-Higgins reasoned that this can only occur when the sediment is in suspension. Because Inman's observations placed the majority of sand transport within the bedload and not the suspended load, the second assumption was also seen as being doubtful. Therefore, Longuet-Higgins (1972) concluded that the coefficient of proportionality K' in equation (4.12) was not as fundamental a relationship as K in equation (4.11).

The two major recent field studies in the area of sediment transport have been carried out by Ingle (1966) and Komar (1969). Their techniques, though suited for high energy environments in warm climates, were modified and adopted for use on Kluane Lake. The major variable which could be quantified by field data collection was the velocity of transport of sediment alongshore. For marking the tracer sediment, Ingle (1966) used a fluorescent dye. This was amply tested and proved to be more akin to the hydraulic properties of the indigenous grains than the painted cobbles, broken brick, or pulverized coal used in other studies. He also advocated its use as a less costly, less dangerous, and more manageable tracer material than radioactive isotopes which had also been widely used in previous studies. The procedure he followed to obtain tracer grain velocities alongshore was

simultaneously to burst plastic bags full of tracer material at different points along the surf-swash zone. Sampling was accomplished by obtaining amounts of surficial sediments at grid points within certain time intervals. The ratio of tracer grains to the total number of grains in the sample was calculated and the average sand advection rate was then established.

In Komar's (1969) field work, the tracer grains were prepared in a similar fashion to Ingle (1966) and similar methods were employed to deduce the sand advection rate, but techniques of tracer injection and sampling were changed. The tracer was introduced to the beachface with a single injection consisting of a trough dug in a direction normal to the shoreline at midtide and filled with the marked sediment. Sampling was done volumetrically at certain grid points in specified time intervals. Because volumes and not surficial readings were taken, an 80 percent return rate of marked sediment was achieved. In addition, measurements of the depth of the mobile layer of sand were taken by two different methods (Komar and Inman, 1970). The first method was based on the assumption that the depth of burial of the tracer in the beachface was equal to the thickness of the mobile bed. Therefore, the buried tracer grains were recovered by the volume samplers, and their depth was measured and recorded. The second method was based on a technique developed by King (1951). It involved a series of small holes which were dug in the beachface at midtide level during low tide and filled with sediment marked with India ink. During the next low tide, the cores were excavated and a depth measurement was taken of the remaining marked particles that were left. The depth measured from the surface of the beachface to the surface of the remaining tracer grains within the original core determined the thickness of the mobile layer. Komar and Inman (1951) reported

the values obtained from both these measures were quite similar.

These procedures were greatly modified for data collection at Kluane Lake because of the prevailing low energy and the temperature of the water. The tracer material was composed of samples taken from the AINA beach. The samples were sieved, and sizes 9, 4, and 2 mm were selected for marking. Different color fluorescent spray paints were used for marking each of the different sized sediments. The spray covered the grains with a thin layer of paint and was assumed to have had a similar effect on its hydraulic properties as a dye. A distance of 2.5, 5, or 10 m, depending upon the magnitude of the wave energy was then measured along the shoreline. After wave and longshore current measurements were recorded, by techniques previously described, the tracer sand was injected into or as close to the breaker zone as possible at one end of the measured distance. The amount of tracer material used also varied with the wave parameters but averaged around 10 grains of 9 mm diameter. Simultaneously with injection, timing of the grains commenced and continued as they were transported to the other end of the measured distance. Approximately 80 percent of the total sample was recorded during each test. The mobile bed thickness was measured only once by the first method of Komar and Inman (1970) because of the limitations previously expressed.

In analysis, equations (4.1) and (4.6) were used for calculation of the energy profile and the immersed weight transport rate respectively. From equations (4.1), (3.3), and (3.6), the wave velocity and the energy density were related to variables which were measured in the field. The variables for the immersed weight transport rate (I) in equation (4.6), however, needs further explanation. The pore space correction factor (p') was given a value

of 0.6 by both Inman and Bagnold (1963) and Komar (1969). This variable is related to the bulk density of sand (ρ_s) and the percent of water contained by the sand ($W\%$) by

$$p' = \frac{W\% \rho_s}{1 + (W\% \rho_s)} \quad (4.19)$$

When values reflecting the composition of the AINA beach sand were substituted for the variables in equation (4.19), the pore correction factor was equal to 0.565, which is close to Komar's value. The derivation and origin of the values for the remaining variables in the volume transport rate (S) in equation (4.10) also need explanation. Since the thickness of the mobile layer of sand (B) was not measured each time the sand advection rate was recorded, it was established from Komar's (1969) data and King's (1972) relationship between wave height and sediment size variables and the mobile bed thickness. This estimation is seen to be as accurate as the empirical field methods required to obtain such data. The values for the tracer grain velocities (\bar{U}_g), the rate of volume transport (S), are included in table (7). The coefficient of proportionality (K) between I and P_1 was determined by equation (4.11) and shown in table (8) with I and P_1 . Its average value varied from 0.36 for 2 mm grains, to 0.40 for 4 mm grains and 0.475 for 2 mm grains. These values are substantially lower than Komar's value of 0.77, but, as Inman and Bagnold (1963) pointed out, very coarse sand beaches, such as the AINA beach, appear to have poorly developed circulation systems. They also add that the

TABLE 7

Tracer grain velocities (\bar{U}_g) and rate of movement
of a volume of sediment over a unit length (S)

DATE		\bar{U}_g (cm/sec)			S ($\text{cm}^3/\text{sec} \times 10^2$)		
		9 mm	4 mm	2 mm	9 mm	4 mm	2 mm
July	5	1.03	0.77	0.61	18.54	13.86	10.98
	5	4.97	2.83	4.72	111.82	636.75	106.20
	8	0.29	0.20	0.25	2.61	1.80	2.25
	9	0.52	0.70	0.45	4.87	6.56	4.22
	11	-	0.18	0.16	-	0.40	0.36
	11	0.33	0.22	0.25	5.94	3.96	4.50
	12	0.30	0.41	0.39	2.70	3.69	3.51
	13	0.50	0.88	0.91	2.25	3.96	4.09
	14	-	0.26	0.49	-	0.23	0.30
	15	0.40	0.31	0.18	3.75	2.90	1.69
	16	-	0.22	0.35	-	0.50	0.79
	18	0.42	0.54	0.57	22.05	28.35	29.92
	19	-	0.10	0.09	-	0.75	0.67
	23	0.08	0.30	0.32	0.36	1.35	1.44
	24	0.32	0.22	0.38	4.80	3.30	5.70
	24	0.15	0.18	0.16	2.81	1.12	3.00
	25	-	0.12	0.20	-	1.08	1.80
	28	0.71	1.02	1.30	5.32	7.65	9.75
	30	-	0.03	0.08	-	0.27	0.72
	30	0.07	0.07	0.11	1.05	1.05	1.65
	31	0.10	0.19	0.17	1.84	3.49	3.12
	31	0.26	0.29	0.35	5.36	5.98	7.22
August	1	1.07	0.99	0.97	9.63	8.91	8.73
	2	0.22	0.59	0.84	1.98	5.31	7.56
	2	0.31	0.85	1.08	4.65	12.75	16.20
	3	1.42	1.47	1.29	90.52	93.71	82.23
	3	0.16	0.13	0.10	10.20	8.29	6.37
	4	0.49	0.11	0.13	3.67	0.82	0.98
	5	0.78	0.61	0.66	4.39	3.87	4.12
	6	0.69	0.47	0.60	3.88	2.64	3.38
	8	0.58	0.84	0.91	2.17	3.15	3.41
	10	0.16	0.13	0.12	0.36	0.29	0.27

TABLE 8

Coefficient of proportionality (K) between immersed weight transport (I) to longshore energy flux (P_1)

DATE 1975		I (dynes/sec x 10^5)			P_1 (ergs/cm sec x 10^5)	K		
		9 mm	4 mm	2 mm		9 mm	4 mm	2 mm
July	5	17.19	12.85	10.18	37.20	0.46	0.34	0.37
	5	103.68	59.04	98.48	73.50	1.41	0.81	1.34
	8	2.42	1.66	2.02	1.47	1.64	1.12	1.38
	9	4.50	6.09	3.92	28.40	0.16	0.64	0.14
	11	-	0.38	0.33	0.14	-	2.67	2.36
	11	5.50	3.66	4.17	21.30	0.26	0.16	0.20
	12	2.50	3.42	3.26	8.61	0.28	0.39	0.38
	13	2.08	3.68	3.79	17.30	0.12	0.21	0.22
	14	-	0.22	0.41	0.61	-	0.36	0.68
	15	3.48	2.70	1.56	2.39	1.46	1.12	0.66
	16	-	0.46	0.73	0.28	-	1.64	2.60
	18	20.44	26.28	27.75	72.90	0.28	0.36	0.38
	19	-	0.69	0.63	3.66	-	0.20	0.16
	23	0.33	1.24	1.34	5.15	0.06	0.24	0.26
	24	4.46	3.06	5.28	9.78	0.45	0.32	0.54
	24	2.60	3.14	2.78	39.70	0.06	0.08	0.08
	25	-	1.00	1.66	6.86	-	0.20	0.24
	28	4.93	7.10	9.04	22.80	0.21	0.32	0.34
	30	-	0.25	0.67	1.33	-	0.18	0.50
	30	0.97	0.97	1.53	22.00	0.04	0.04	0.08
31	1.71	3.24	2.89	15.80	0.57	0.21	0.18	
31	4.98	5.55	6.69	33.50	0.15	0.16	0.20	
August	1	8.92	8.26	8.10	8.32	1.06	0.99	0.98
	2	1.83	4.92	7.00	5.03	0.36	0.98	1.40
	2	4.30	11.82	15.02	36.10	0.12	0.33	0.42
	3	83.94	28.96	76.26	261.00	0.32	0.33	0.30
	3	9.45	7.68	5.91	113.00	0.09	0.06	0.04
	4	3.40	0.76	0.90	6.15	0.56	0.12	0.15
	5	4.06	3.60	3.44	21.90	0.18	0.16	0.15
	6	3.60	2.44	3.14	21.40	0.16	0.12	0.15
	8	2.01	2.92	3.16	12.50	0.16	0.22	0.26
	10	0.33	0.27	0.26	4.56	0.08	0.06	0.04

"theoretical relations refer to conditions well above the threshold of bed movement and therefore to a constant maximum value of which K is supposed to rise. At the threshold of sediment movement, K is clearly equal to zero. If the field data leading to empirical transport rates include threshold and subthreshold wave conditions, then the calculated values of K will be lower than those for fully developed transport." (Inman and Bagnold, 1963, p. 547)

To determine the type of relationship that exists between threshold and steady conditions of K, three graphs were plotted each with values of one of the tracer grain sizes. These graphs (Figures 15, 16, 17) depict a curvilinear relationship of K which was accounted for by Komar (1969) in stating,

". . . for lower values of P_1 , equation ($I = 0.80 P_1 + 2.5 \times 10^4$) would no longer be valid and the curve of I versus P_1 would depart from a straight line and would curve downward through the origin." (p. 64)

As shown by the graphs, when the value of P_1 approaches that of Komar's, the relationship does hold as a straight line. Therefore, equation (4.11), although developed in high-energy marine conditions, does hold for lower-energy lacustrine conditions. In addition, when sediment transport is less than steady state, the curvilinear relationship that develops between I and P_1 could be the result of the increased importance of such factors as the hypothetical coefficient of friction (C_f') as hinted at by Longuet-Higgins (1972).

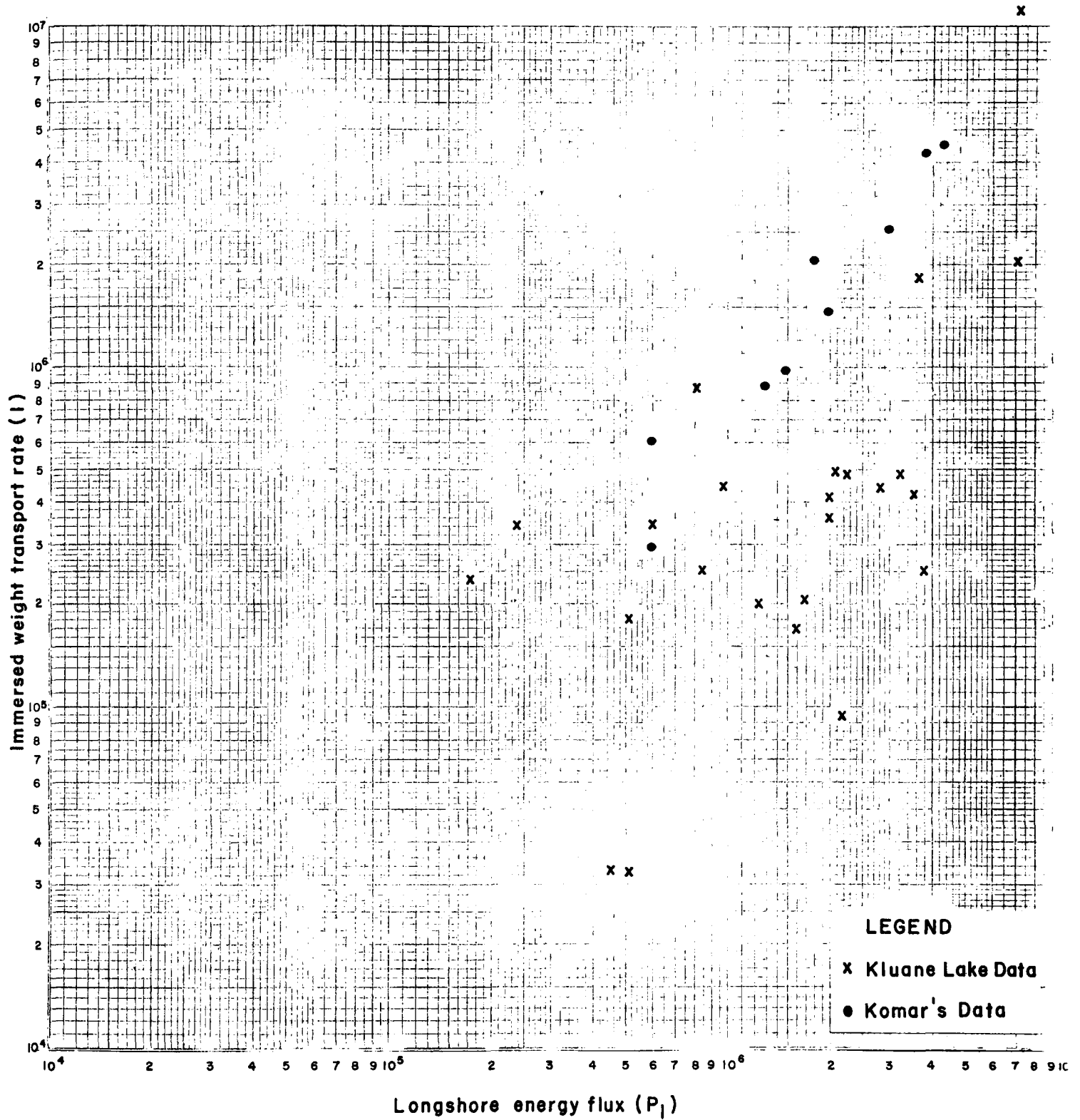


FIGURE.15 RELATIONSHIP BETWEEN IMMERSED WEIGHT TRANSPORT RATE AND LONGSHORE ENERGY FLUX. 9mm.SEDIMENT SIZE.

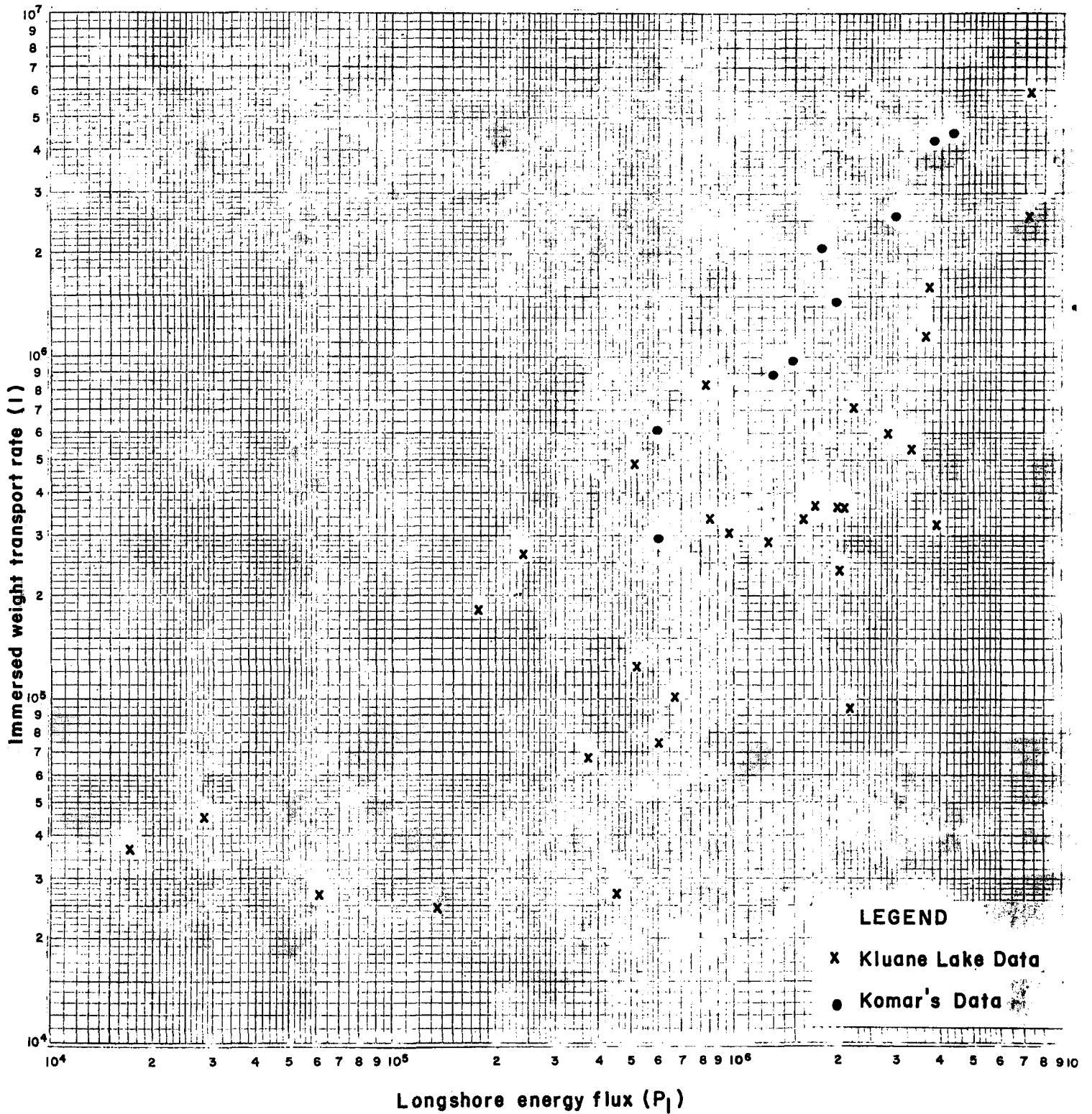


FIGURE.16 RELATIONSHIP BETWEEN IMMERSED WEIGHT TRANSPORT RATE AND LONGSHORE ENERGY FLUX. 4 mm. SEDIMENT SIZE.

5. CONCLUSIONS

From this study of sediment movement under both ice and wave conditions at Kluane Lake, a number of conclusions can be drawn. During the 1975 season of ice break up, various sediment disturbance features were observed, recorded, and compared with features described in the literature of both marine and lacustrine environments. These include evidence of kaimoo build up, ice-rafted sediment, inverse ice-contact cusps, longshore movement of sediment by grounding ice floes, beach pitting, and ice-push ridges. These features, however, had much less permanent effect on the beach form than in such arctic marine environments as described by Hume and Schalk (1973) at Point Barrow, Alaska. The reasons for this variance lie in differing amounts of wind energy and ice between the two areas, and the dramatic rise in the Kluane Lake water level during the summer months which erases all evidence of surficial sediment disturbance by ice. The major limitation of the descriptive data presented in this study is that only one break up season was observed. To obtain a better appreciation of the processes of sediment inclusion and disturbance by ice, both freeze up and break up should be observed. In addition, observation should be done over a number of years to lower the probability of recording an unusual year. Only then can attempts to reach definitive conclusions on how ice affects the beach sediments of Kluane Lake and how it differs from other environments be justified.

The development of a **longshore current velocity prediction equation** has culminated in the work done by Longuet-Higgins (1970a, b, 1972) resulting in the relationship expressed by equation (3.19). Within his analysis, Longuet-Higgins assumed the coefficient of friction (C_f) to have nearly a constant value averaging around 0.01. This value, however, did not fit the data collected at Kluane Lake. Based on Schlichting's (1955) interpolative equation for C_f , developed from results of Nikuradse's experiments with roughened pipes (equation, 3.20), the corrected values of C_f were found to vary from a low of 0.0118 to a high of 0.0340 for corresponding wave energies of 73.5×10^5 and 4.56×10^5 ergs/cm sec respectively. This range of values of C_f with respect to longshore wave energy emphasizes the relative importance of this parameter with lower-energy environments. Further proof of the increased importance of this variable is depicted in graphs where the observed longshore current velocity is plotted against the predicted longshore current velocity. With the value of C_f fixed at 0.01, a nearly perfect correlation occurs around a line with a slope of 0.615, but with varying values of C_f determined from equation (3.19), a nearly perfect correlation occurs around a line of **0.916**. Therefore, in the case of Kluane Lake, more accurate predictions can be made with equation (3.18) if the values of the coefficient of friction are more sensitive to the local environment. However, many more tests will have to be carried out on beaches composed of varying sized sediment particles and differing wave energy environments to verify this further.

From Komar's (1969) analysis of his field data, he found that the coefficient of proportionality (K) between the immersed weight transport rate and the wave energy flux alongshore was equal to 0.77 when longshore

sediment transport approached steady state conditions. He also pointed out that this linear value for K was not sustained when less than steady state conditions prevailed, but curved downward to the threshold. Inman and Bagnold (1963) further implied that the nearshore circulation system would be less well developed on beaches composed of coarse sediments. Data on both sediment transport rate and longshore energy flux of waves collected at the AINA beach, a coarse sand beach, show further confirmation of both these points. When the immersed weight transport rate (I) is plotted against the longshore energy flux (P_1), figures (15, 16, 19) showed that a linear relationship develops when the values of I and P_1 become close to those collected by Komar (1969). When these values decrease, the relationship becomes curvilinear, curving downward to the threshold energy. Because of the coarse sand composition of the beach, K rarely exceeds Komar's value and is more often lower than it. The limitations of further interpretation of these relationships lie in the accuracy in acquiring the values of the necessary parameters in the field. The values of the depth of the mobile layer and the width of the foreshore zone, for example, were interpolated from preexisting data and observed at the site respectively. Therefore, one consideration for further work in longshore sediment movement could be the determination of a more accurate relationship between grain diameter size and wave energy and the depth of the mobile layer. One other area for further research could be understanding the various parameters which influence the curvilinear relationship for values of K between the threshold and steady state, and their empirical relationship which determine the magnitude of the curve. From this, a more accurate equation can be developed for predicting the rate of longshore sediment movement under a wide range of wave energies on beaches composed of varying sized sediments.

REFERENCES

- Bagnold, R.A. (1963) "Mechanics of marine sedimentation", The Sea, vol. 3, ed. M.N. Hill, Interscience Publ., New York, pp. 507-528.
- Balsillie, J.H. (1975) "Surf observations and longshore current prediction", U.S. Army Coastal Eng. Res. Center Tech. Memo., no. 58, 39 pp.
- Battjes, J.A. (1975) "Modeling of turbulence in the surf zone", Symposium on Modeling Techniques, Second Ann. Symp. of Waterways, Harbors, and Coastal Eng., Div. of A.S.C.E., San Fransisco, Calif., vol. 2, pp. 1050-1061.
- Bostock, H.S. (1952) "Geology of northwest Shawkak Valley, Yukon Territory", Canada Geol. Surv. Mem., no. 267, 54 pp.
- _____. (1969) "Kluane Lake, Yukon Territory, its drainage and allied problems", Can. Geol. Surv. Paper, no. 69-28, 19 pp.
- Brebner, A. and J.W. Kamphuis, (1963) "Model tests on relationship between deep-water wave characteristics and longshore currents", Queens University Civil Eng. Res. Rep. 31, pp. 1-25.
- Bryan, M.L. (1970) "Sedimentation in Kluane Lake, Yukon Territory, Canada", A.A.G. Proceedings, vol. 2, pp. 31-35.
- _____. (1971) "Sedimentation in glacially fed Kluane Lake, Yukon Territory, Canada", unpublished thesis, Univ. of Michigan, Ann Arbor, Mich., 203 pp.
- Bryan, M.L. and M.G. Marcus. (1972) "Physical characteristics of nearshore ice ridges", Arctic, vol. 25, no. 3, pp. 182-192.
- Bruun, P. (1963) "Longshore currents and troughs", J. of Geophys. Res., vol. 68, pp. 1065-1078.
- Butkovich, T.R. (1955) "The crushing strength of ice", SIPRE Res. Paper no. 15, 5 pp.
- Caldwell, J.M. (1956) "Wave action and sand movement near Anaheim Bay, California", U.S. Army Beach Erosion Board, Tech. Memo., no. 68, 21 pp.
- Davis, R.A. (1973) "Coastal ice formation and its effect on beach sedimentation", Shore and Beach, vol. 41, iss. 1, pp. 3-9.

- DeVries, M. (1971) "On the applicability of fluorescent tracers in sedimentology", Delft Hydraulics Laboratory, Publication no. 94, 19 pp.
- Denton, G.H. and M. Stuiver. (1966) "Neoglacial chronology, northeastern St. Elias Mountains, Canada", *Am. J. of Sc.*, vol. 264, pp. 577-599.
- Dionne, J.C. (1972) "Ribbed grooves and tracks in mud tidal flats of cold regions", *J. of Sed. Pet.*, vol. 42, pp. 848-851.
- Dionne, J.C. and C. Laverdière. (1972) "Ice formed beach features from Lake St. Jean, Quebec", *Can. J. of Earth Sci.*, vol. 9, no. 8, pp. 979-990.
- Doeglas, D.J. (1955) "The origin and destruction of beach ridges", *Leidse Geologische Mededelingen, Deel 20*.
- Fahnestock, R.K. (1969) "Morphology of the Slims River", IRRP Scientific Results, vol. 1, pp. 161-172.
- Galvin, C.J. Jr. (1967) "Longshore current velocity: a review of theory and data", *Rev. of Geophys.*, vol. 5, no. 3, pp. 287-304.
- _____. (1968) "Breaker type classification on three laboratory beaches", *J. of Geophys. Res.*, vol. 73, no. 12, pp. 3651-3659.
- Galvin, C.J. Jr. and R.P. Savage. "Longshore currents at Nags Head, North Carolina", U.S. Army Coastal Eng. Res. Center Bull., no. 11, pp. 11-29.
- Gilbert, G.K. (1890) "Lake Bonneville", U.S. Geol. Survey Monographs, vol. 1, 438 pp.
- Goldthwait, L. (1957) "Ice action on New England lakes", *J. of Geol.*, vol. 3, pp. 99-103.
- Grant, U.S. (1943) "Waves as a sand transporting agent", *Am. J. of Sci.*, vol. 241, pp. 402-421.
- Greene, H.G. (1970) "Microrelief of an arctic beach", *J. of Sed. Pet.*, vol. 40, no. 1, pp. 419-427.
- Hare, F.K. and M.R. Thomas (1974) *Climate Canada*, Wiley Publishers of Canada Ltd., Toronto, Ontario, 256 pp.
- Harrison, W. and W.C. Krumbein. (1964) "Interactions of the beach - ocean - atmosphere system at Virginia Beach", U.S. Army Coastal Eng. Res. Center, Tech. Memo., no. 7, pp. 1-102.

- Hume, J.D. and M. Schalk. (1964) "The effects of ice push on arctic beaches", *Am. J. of Sci.*, vol. 262, pp. 267-273.
- _____. (1967) "Shoreline processes near Barrow, Alaska: a comparison of the normal and catastrophic", *Arctic*, vol. 20, pp. 86-103.
- _____. (1973) "The effects of ice on the beach and nearshore, Point Barrow, Arctic Alaska", Subcontract ONR-413, 413a2, AINA, 25 p.
- Ingle, J.C. Jr. (1966) The Movement of Beach Sand, Developments in sedimentology, vol. 5, Elsevier Publ. Co., New York, 221 p.
- Inman, D.L. (1949) "Sorting of sediments in the light of fluid mechanics", *J. of Sed. Pet.*, vol. 19, no. 2, pp. 51-70.
- Inman, D.L. and W.H. Quinn. (1952) "Currents in the surf zone", Proc. Second Conf. Coastal Engr., Council Wave Res., Univ. of California, pp. 24-36.
- Inman, D.L. and R.A. Bagnold. (1963) "Littoral Processes", The Sea, vol. 3, ed. M.N. Hill, Interscience Publ., New York, pp. 529-553.
- Jennings, J.N. (1958) "Ice action on lakes", *J. Glaciology*, vol. 3, no. 23, pp. 228-229.
- Johnson, D.W. (1919) Shore Processes and Shoreline Development, Hafner Publ., New York, 584 pp.
- Johnson, J.W. (1956) "Dynamics of nearshore sediment movement", *Bull. Am. Ass. Pet. Geol.*, vol. 40, pp. 2211-2232.
- Kidson, C. and A.P. Carr. (1959) "The movement of shingle over the seabed close inshore", *Geog. J.*, vol. 125, parts 3-4, pp. 380-384.
- King, C.A.M. (1951) "Depth of disturbance of sand on sea beaches by waves", *J. Sed. Pet.*, vol. 21, pp. 131-140.
- _____. (1966) Techniques in Geomorphology, Edward Arnold Ltd., London, England, 342 pp.
- _____. (1972) Beaches and Coasts, Edward Arnold Ltd., London, England, 570 pp.
- Komar, P.D. (1969) "The longshore transport of sand on beaches", unpublished Ph. D. Thesis, University of California, San Diego, Calif., 143 pp.

- _____. (1971) "The mechanics of sand transport on beaches",
J. Geophys. Res., vol. 76, no. 3, pp. 713-721.
- Komar, P.D. and D.L. Inman. (1970) "Longshore sand transport on beaches",
J. Geophys. Res. vol. 75, no. 30, pp. 5914-5927.
- Longuet-Higgins, M.S. (1970a) "Longshore currents generated by obliquely
incident sea waves 1", J. Geophys. Res., vol. 75, no. 33,
pp. 6778-6789.
- _____. (1970b) "Longshore currents generated by obliquely
incident sea waves 2", J. Geophys. Res., vol. 75, no. 33,
pp. 6790-6801.
- _____. (1972) "Recent progress in the study of longshore
currents", Waves on Beaches, ed. R.E. Meyer, pp. 203-248.
- Longuet-Higgins, M.S. and R.W. Stewart. (1964) "Radiation stresses in
water waves; a physical discussion with applications",
Deep-sea Res., vol. 11, pp. 529-562.
- Marsh, W.M., B.D. Marsh and J. Dozier. (1973) "Formation, structure, and
geomorphic influence of Lake Superior icefoots", Am. J. Sci.,
vol. 273, pp. 48-64.
- McCann S.B. and R.J. Carlisle. (1972) "The nature of the icefoot on the
beaches of Radstock Bay", Inst. British Geog. Spec. Publ.,
no. 4, pp. 175-186.
- Moore, G.W. (1966) "Arctic beach sedimentation", Environment of the Cape
Thompson Region, Alaska, eds. Wilimovski, N.J., and Wolfe,
J.N., U.S. Atomic Energy Comm., Div. Tech. Inf., pp. 587-608.
- Motyka, J.M. and D.H. Willis. (1975) "Alongshore sediment transport due
to variations in wave height", Hydraulic Res. Center Notes,
no. 17, pp. 6-7.
- Muller, J.E. (1958) "Kluane Lake map-area, Yukon Territory", Can. Geol.
Surv. Paper, no. 58-9.
- Nichols, R.L. (1953) "Marine and lacustrine ice-pushed ridges", J. of
Glaciology, vol. 2, no. 13, pp. 172-175.
- _____. (1961) "Characteristics of beaches found in polar climates",
Am. J. Sci., vol. 251, pp. 694-708.
- Nickling, W.G. (1975) "Eolian sediment transport, Slims River Valley,
Yukon Territory", unpublished Ph. D. Thesis, University
of Ottawa, Ottawa, Ontario.

- Patrick, D.A. and R.L. Wiegell. "Amphibious tractors in the surf", Proc. First Conf. Ships and Waves, Council Wave Res., pp. 397-422.
- Phillips, O.M. (1957) "On generation of waves by turbulent wind", J. of Fluid Mech., vol. 2, no. 5, pp. 417-445.
- Prandtl, L. (1952) Essentials of Fluid Dynamics, Hafner Publ. Co., New York, 452 pp.
- Putnam, J.A., Munk W.H. and Traylor, M.A. (1949) "The prediction of longshore currents", Trans. Am. Geophys. Union, vol. 30, no. 3, pp. 337-345.
- Rex, R.W. (1955) "Microrelief produced by sea ice grounding in the Chuckchi Sea near Barrow Alaska", Arctic, vol. 8, no. 3, pp. 135-141.
- _____. (1964) "Arctic Beaches, Barrow Alaska", Papers in Marine Geology (Shepard Commemorative Volume), ed. R.L. Miller, McMillan Co., New York, pp. 384-401.
- Savage, R.P. (1959) "Laboratory study of the effect of grains on the rate of littoral transport", U.S. Army Beach Erosion Board, Tech. Memo., no. 14, 55 p.
- Schlichting, H. (1955) Boundary Layer Theory, McGraw-Hill Book Co. Inc., New York, 535 pp.
- Scott, I.D. (1927) "Ice push on lakes", Papers Mich. Acad., vol. 7, pp. 107-123.
- Shepard, F.P. and D.L. Inman. (1951) "Nearshore Circulation", Proc. First Conf. Coastal Eng., Council Wave Res., pp. 50-59.
- Shore Protection Manual Volume I, (1973) U.S. Army Coastal Eng. Res. Center, 498 pp.
- Short, A.D. and W.J. Wiseman Jr. (1975) "Coastal breakup in the Alaskan Arctic", Bull. Geol. Soc. Am., vol. 86, iss. 2, pp. 199-202.
- Sundberg-Falkenmark, M. (1957) "Studies on lake-ice movements", Toronto Ass. Int. D'Hydrologie Scientifique, vol. 4, pp. 266-279.
- Tanner, W.F. (1973) "Advances in nearshore physical sedimentology: a selective review", Shore and Beach, pp. 22-27.
- Taylor-Barge, B. (1969) "Summer climate of the St. Elias Mountains Regions", IRRP Scientific Results, vol. 1, pp. 3-49.
- Wagner, W.P. (1970) "Ice movement and shoreline modification, Lake Champlain, Vermont", Bull. Geol. Soc. Am., vol. 81, no. 1, pp. 117-126.

Wiegand, R.L. (1964) Oceanographic Engineering, Fluid Mechanics Series, Prentice Hall, New Jersey, 325 pp.

Wilson, J.T., J.H. Zumberge and E.W. Marshall. (1954) "A study of ice on an inland lake", SPIRE project 2030, Report 5, part 1, 78 pp.